to be no more than $10^7 cm^2/s$. Otherwise, the
by overestimating horizontal mixing.
cator of equatorial gradient currents; moreover
here than in nonequatorial regions. The wind
f the sea surface currents, but its effect fades
at the level of 100-150 m.

is paper was discussed at the seminars of GFDL of
ty. The authors are grateful to George Veronis, Kirk
l comments.

FERENCES
kov. 1975. Surface topography of the Atlantic Ocean.
al model of the world ocean: preliminary results.
n. Proceedings Symposium held in Durham, N. H.,
Sciences, Washington, D.C.
n the calculation of currents in a basin comprising
Atmos. i Okeana. 10(11), 1194–1207.
ulation of currents in the Tropical Atlantic. *Mete-*
l and calculation of currents in Equatorial Atlantic.
eana. 11(5), 534–537.
rrents, *in* Numerical Models of Ocean Circulation,
1–204.
. A numerical calculation of the circulation in the
2, 336–354.
s and observations of the Cromwell current. J. Mar.
al Mathematics. Publishing House "Nauka," Siberian
72. Exact solutions of certain transformed dynamic
Nauk SSSR, Fiz. Atmos. i Okeana., *10*, 1073–1079.
ations of ocean currents. Translation available from
National Science Foundation, Washington, D.C.
lculation of currents in an oceanic basin, including
MGI *Akad. Nauk* Ukr. SSR, Sevastopol.
a large-scale oceanic circulation, *in* The Sea, v. *VI*,
ohn Wiley & Sons.
The density field as the main indicator of steady sea
nos. i Okeana, *6*, 64–76.
4. On some results of the diagnostic calculations of
z. Issled., *3*, MGI *Akad. Nauk Ukr.* SSR, Sevastopol.
rodynamic characteristics in the Gulf Stream region
SSR, Fiz. Atmos. i Okeana, *11*, 93–95.
i wind stress in the equatorial region of the Atlantic
rrent. Kiev, Naukova Dumka, 141–153.
977.

A model of phytoplankton plume formation during variable Oregon upwelling

by J. S. Wroblewski[1,2]

ABSTRACT

A time dependent, two-dimensional, marine ecosystem model relates wind events, upwelling, and primary production off the Oregon coast. Model predictions of daily primary production (mg N m^{-2} day^{-1}) increase soon after an intensification of the northerly component of the wind stress. Paradoxically the highest phytoplankton concentration occurs upon relaxation of winds after a major upwelling event. When northerly winds are strong, phytoplankton are supplied with limiting nutrient but the cells experience a short euphotic zone residence time. The phytoplankton are advected offshore and down to light limiting depths by the lower, cyclonically rotating gyre of a two-cell, zonal circulation. After relaxation of the wind, downwelling is not as prevalent and the plants remain longer in the nutrient-rich, lighted zone.

The ecosystem dependent variables (phytoplankton nitrogen, zooplankton nitrogen, nitrate, ammonia and detrital nitrogen) are advected by an explicitly modeled flow which is influenced by bottom topography and a variable wind stress. Simulations predict a phytoplankton and detritus plume for which considerable observational evidence exists. It is concluded that during summer, advection by a two-cell, upwelling circulation is the major physical mechanism leading to mesoscale patchiness in the plankton and nutrient fields.

1. Introduction

During the season favorable for coastal upwelling off the western boundary of continents, the local circulation is strongly influenced by occasional wind events of several days duration. Variability in the wind stress affects the rate of upwelling and, indirectly, the local primary productivity.

Primary production is a function of the availability of light and nutrients, and its rate is governed by temperature. Because the physical and chemical environments in a coastal upwelling region are highly variable, production must be investigated within a temporal, spatial framework. Smayda (1966) had only limited success in predicting daily primary production in the Gulf of Panama from an empirical equation relating phytoplankton biomass directly to the wind stress and surface temperature. Small *et al.* (1972) concluded that there was no simple empirical re-

1. Department of Oceanography, Florida State University, Tallahassee, Florida, 32306, U.S.A.
2. Present address: Department of Oceanography, Dalhousie University, Halifax, Nova Scotia, B3H 4J1, Canada.

lationship between daily primary production off Oregon and such environmental factors as incident radiation, photic depth or rate of upwelling. Nonspatial, upwelling ecosystem models (e.g. Cushing, 1971) are useful for relating productivity to nutrient concentration, light and herbivore grazing intensity, but they neglect the variability of the environment. Walsh and Dugdale (1971) and Walsh (1975) have pioneered the construction of spatial models of upwelling ecosystems.

This paper is the first attempt at coupling a complex model of primary productivity with a time dependent, numerical model of an upwelling circulation. Its purpose is to determine whether our current understanding of coastal upwelling and marine biological processes can be combined into a dynamical explanation of the phytoplankton distribution off Oregon during the upwelling season. Nonlinear equations for the distribution of phytoplankton nitrogen, herbivore nitrogen, detrital nitrogen, and the nutrients, nitrate and ammonia in a transverse plane normal to the Oregon coast are solved numerically for both continuous and intermittent upwelling conditions. Daily primary production of the water column is calculated at 1 km intervals within 50 km of the coast. The flow field is driven in one case by a theoretical wind stress. In a second case, daily primary production is computed using a flow field driven by winds recorded by an anemometer at Newport, Oregon. Model solutions are compared with data collected off the Oregon coast in 1972 and 1973 during the Coastal Upwelling Experiment. CUE was part of the Coastal Upwelling Ecosystems Analysis Program sponsored by IDOE.

The ecosystem dynamics are formulated in Section 2. These equations are investigated first neglecting advection and all horizontal dependence. The steady state, vertical solutions of these equations are utilized as initial conditions for the time dependent, two-dimensional, upwelling ecosystem model. In Section 3, the explicitly modeled upwelling circulation, the numerical scheme, and the boundary conditions are discussed. In Section 4 predicted water column productivities and simulated distributions of the plankton and nutrient fields are compared to observations. Important questions concerning poorly known, biological parameter values and controversial process formulations are discussed in view of an empirical sensitivity analysis. Finally, the ability of the model to predict the distribution of nitrogen during upwelling off Oregon is evaluated.

2. Model formulation—the biological dynamics

a. The phytoplankton equation. Let us begin with a parameterization of physical and biological processes interacting in the ocean. The general equation describing the distribution of a nonconservative variable (e.g. phytoplankton biomass, P) in the sea is

$$\frac{\partial P}{\partial t} + \nabla \cdot \vec{V} P - \nabla \cdot (K \nabla P) = \text{biological dynamics} \qquad (1)$$

oduction off Oregon and such environment
epth or rate of upwelling. Nonspatial, upwel
1971) are useful for relating productivity t
bivore grazing intensity, but they neglect th
and Dugdale (1971) and Walsh (1975) hav
nodels of upwelling ecosystems.

oupling a complex model of primary produc
al model of an upwelling circulation. Its pur
rrent understanding of coastal upwelling and
ombined into a dynamical explanation of the
on during the upwelling season. Nonlinear
plankton nitrogen, herbivore nitrogen, detrital
nd ammonia in a transverse plane normal to
ally for both continuous and intermittent up
duction of the water column is calculated at
ast. The flow field is driven in one case by a
case, daily primary production is computed
rded by an anemometer at Newport, Oregon.
data collected off the Oregon coast in 1972
ng Experiment. CUE was part of the Coastal
m sponsored by IDOE.

ulated in Section 2. These equations are in
and all horizontal dependence. The steady
ions are utilized as initial conditions for the
welling ecosystem model. In Section 3, the
on, the numerical scheme, and the boundary
4 predicted water column productivities and
n and nutrient fields are compared to obser
ng poorly known, biological parameter values
are discussed in view of an empirical sensi
he model to predict the distribution of nitro
uated.

ynamics

us begin with a parameterization of physical
the ocean. The general equation describing
variable (e.g. phytoplankton biomass, P) in

$K\nabla P) =$ biological dynamics (1)

where t is time, $\vec{V}$ represents the horizontal and vertical water velocities, and K is the coefficient of eddy diffusivity. The first term is the local change in P, the second represents advection of P, and the third represents turbulent mixing. "Biological dynamics" refers to the biological processes affecting the local change in P. Phytoplankton biomass is expressed in units of concentration of nitrogen, the biologically limiting nutrient off Oregon (Park, 1967). Biological rates are expressed in terms of nitrogen turnover time (μg at N l^{-1} hr^{-1}).

Three fundamental assumptions are necessary to reduce (1) to tractable form: 1) the velocity field is assumed to be nondivergent, $\nabla \cdot \vec{V} = 0$, a requirement for conservation of mass; 2) the horizontal and vertical coefficients of eddy diffusivity are assumed constant; and 3) all derivatives in the longshore direction are neglected. The region of the Oregon coast chosen for the major field experiment CUE is an area where this assumption is more likely to be valid than other upwelling regions currently under study. In a coordinate system in which y is in the longshore direction, x is positive toward the coast, and z is positive downward, (1) can be rewritten

$$\frac{\partial P}{\partial t} + u\frac{\partial P}{\partial x} + w\frac{\partial P}{\partial z} - K_h\frac{\partial^2 P}{\partial x^2} - K_v\frac{\partial^2 P}{\partial z^2} = \text{biological dynamics} \qquad (2)$$

The horizontal velocity, u, is positive toward the coast, and the vertical velocity, w, is positive upward.

Equations similar to (2) are written for the other model dependent variables: herbivore nitrogen, Z; detrital nitrogen, D; nitrate[3], NO_3; and ammonia, NH_4. Carnivore biomass or predation is not considered.

The biological dynamics included in (2) describe growth of P, grazing upon P by herbivores, Z, and lysis of senescent P cells. Multiple nutrient limitation of phytoplankton growth is restricted to the dissolved nutrients, nitrate and ammonia. It is assumed extracellular excretion of nitrogen by growing plants is negligible. Plant growth inhibition or enhancement by trace elements and chelation effects (Johnston, 1964; Barber and Ryther, 1969) are not considered.

The biological dynamics affecting the local change in P are written

$$\frac{\partial P}{\partial t} = V_m f(I,T)\left[\frac{NO_3}{k_u+NO_3}e^{-\Psi NH_4} + \frac{NH_4}{k_u+NH_4}\right]P - R_m\left[1 - e^{-\Lambda(P-Pt)}\right]Z - \Xi P \qquad (3)$$

where

$$f(I,T) = \left[\frac{I/I_s}{[1+(I/I_s)^2]^{1/2}\,[1+(\theta I/I_s)^2]^{\eta/2}}\right](ab^{cT}) .$$

Dugdale (1967), Eppley and Coatsworth (1968), MacIsaac and Dugdale (1969), and Caperon and Meyer (1972) have demonstrated that uptake rates of nitrate and

3. The charges on the ions NO_3^- and NH_4^+ are omitted for convenience.

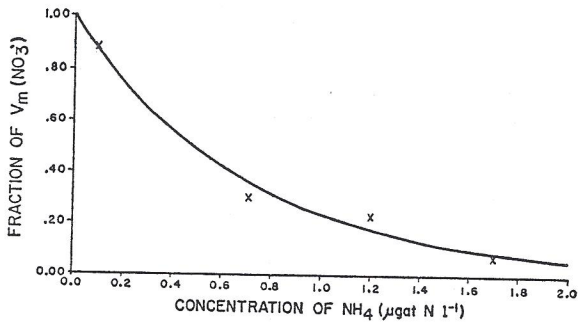

Figure 1. A least squares fit of the function, $V/V_m(NO_3) = e^{-\Psi NH_4}$ to the data of Walsh and Dugdale (1972), giving $\Psi = 1.462$ (μg at $NH_4/l)^{-1}$.

ammonia by marine phytoplankton can be expressed as hyperbolic functions of nutrient concentration when that nutrient limits growth. The Michaelis-Menton formulation describing these uptake kinetics is

$$V = \frac{V_m N}{k_u + N}$$

where V is the uptake rate (time^{-1}) of nutrient N (concentration), V_m is the maximum uptake rate, and k_u is the Michaelis or half-saturation constant. The concentration k_u supports half the maximum uptake rate. The assumption is made that nutrient uptake is equivalent to cell growth. This is justifiable when modeling phytoplankton growth in upwelled waters.

Phytoplankton cells preferentially take up ammonia over nitrate. The presence of ammonia inhibits the activity of the enzyme, nitrate reductase, essential to the uptake kinetics (Packard and Blasco, 1974) and acts by reducing V_m (NO_3) (Dugdale and MacIsaac, 1971; Walsh and Dugdale, 1972). To simulate suppression of nitrate uptake by ammonia, V_m (NO_3) is multiplied by the exponential, $e^{-\Psi NH_4}$. Figure 1 shows this exponential reduction in V_m (NO_3) with increasing ammonia concentration fitted to the data of Walsh and Dugdale (1972).

In Figure 2 the theoretical uptake rates of nitrate and ammonia are shown for increasing concentrations of NO_3 and NH_4. Total nitrogen uptake by phytoplankton is given by

$$V = V_m \left[\frac{NO_3}{k_u + NO_3} \, e^{-\Psi NH_4} + \frac{NH_4}{k_u + NH_4} \right]$$

where it has been assumed V_m (NO_3) = V_m (NH_4) and the half-saturation constants, k_u, for nitrate and ammonia are equal (Eppley *et al.*, 1969; MacIsaac and Dugdale, 1969).

In addition to nutrient concentration, the growth rate of phytoplankton is influenced by temperature and light intensity. I have chosen to model phytoplankton growth as a multiplicative factor of nutrients, light, and temperature. Walsh (1975)

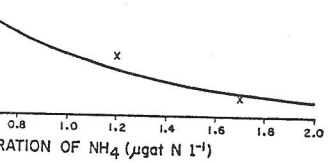

n, $V/V_m(NO_3) = e^{-\Psi NH_4}$ to the data of Walsh and $H_4/l)^{-1}$.

an be expressed as hyperbolic functions of rient limits growth. The Michaelis-Menton etics is

$$= \frac{V_m N}{k_u + N}$$

nutrient N (concentration), V_m is the maxi- elis or half-saturation constant. The concen- uptake rate. The assumption is made that growth. This is justifiable when modeling rs.

ke up ammonia over nitrate. The presence enzyme, nitrate reductase, essential to the 974) and acts by reducing V_m (NO_3) (Dug- Dugdale, 1972). To simulate suppression of is multiplied by the exponential, $e^{-\Psi NH_4}$, ion in V_m (NO_3) with increasing ammonia and Dugdale (1972).

ates of nitrate and ammonia are shown for H_4. Total nitrogen uptake by phytoplankton

$$e^{-\Psi NH_4} + \frac{NH_4}{k_u + NH_4}\Bigg]$$

V_m (NH_4) and the half-saturation constants, Eppley *et al.*, 1969; MacIsaac and Dugdale,

, the growth rate of phytoplankton is in- ity. I have chosen to model phytoplankton ents, light, and temperature. Walsh (1975)

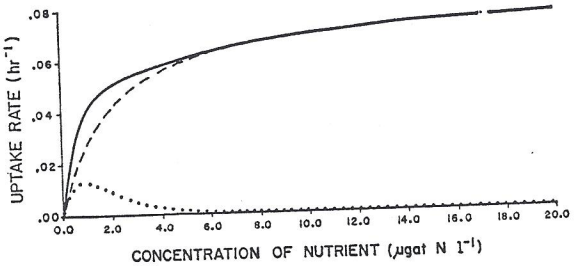

Figure 2. Uptake rate of nitrate (dotted line), ammonia (dashed line) and total nitrogen uptake (solid line) with increasing concentration of NO_3 and NH_4. 10 μg at N l^{-1} on the abscissa means 5 μg atom of each ionic form are present in solution. Uptake of NO_3 is inhibited by NH_4 in a manner formulated in the text.

regarded a single factor as growth limiting. However, Parsons and Takahashi (1973) and Platt *et al.* (1977) suggest primary production in the sea is regulated simultaneously by several environmental variables.

The response of phytoplankton growth to light is described by the so-called "photosynthesis vs. light intensity" or P_h vs. I curve (Parsons and Takahashi, 1973). Because the maximum rate of photosynthesis, P_m, depends on an optimum temperature, nutrient and light regime, plots of P_h vs. I are normalized by P_m (Yentsch and Lee, 1966). Equating relative photosynthesis with relative nutrient uptake, V/V_m, a modification of the formulation by Vollenweider (1965),

$$\frac{P_h}{P_{opt}} = \frac{I/I_s}{[1 + (I/I_s)^2]^{1/2}\,[1 + (\theta I/I_s)^2]^{\eta/2}},$$

is used to describe the rate of phytoplankton growth as a function of light intensity, I (cal cm^{-2} min^{-1}). I_s is the irradiance for which $P_h = P_{opt}\,[2(1 + \theta^2)^\eta]^{-\frac{1}{2}}$. P_{opt} is the maximum photosynthetic rate, P_m, multiplied by a function of θ and η (see Fee, 1969). This complex formulation is adopted here because of its ability to fit P_h vs. I curves exhibiting photoinhibition.

Photosynthetically active light intensity, as a function of time and depth, is written

$$I(z,t) = 0.5\, I_m \sin\left[\frac{\pi \bmod (t,24)}{d}\right] e^{-[\kappa_w z + \kappa_p \int_0^z P(z)dz]} \qquad (4)$$

where I_m (cal cm^{-2} min^{-1}) is the light intensity immediately below the sea surface at local apparent noon, d is the daylength fraction of a day, κ_w (cm^{-1}) is the extinction coefficient of the local seawater in the absence of any phytoplankton (Platt *et al.*, 1977), κ_p (cm^2/μg at N) is the extinction coefficient per unit concentration of phytoplankton, and $P(z)$ is the concentration (μg at N cm^{-3}) of phytoplankton at depth z (cm). When the sine function becomes negative, I is set equal to zero. Periodicity is enforced by the modulo, whereby the sine function is reset to zero at the beginning of the day.

A sine function was chosen to express the variation of light with time of day as it fits insolation data recorded on a surface buoy 13 km off Sand Lake, Oregon during CUE (Reed and Halpern, 1974). Light attenuation with depth in the ocean follows the well-known Beers-Lambert law. Self-shading of the phytoplankton is expressed as the second part of the exponential in (4).

Where photosynthesis is light saturated and nutrients are not limiting, the rate of plant growth may be a direct function of temperature (Winter *et al.*, 1975). Eppley (1972) found under these conditions the specific growth rate μ (doublings day^{-1}) could be predicted from the empirically derived equation,

$$\mu = ab^{cT}$$

where a is 0.851 doublings day^{-1}, b is the constant 1.066, c is 1°C^{-1}, and T is temperature (°C).

Most marine phytoplankton experience a suppression of the growth rate above some optimum temperature. As temperatures are usually less than this optimum in an upwelling region, Eppley's empirical relationship is adequate for modelling purposes here. Phytoplankton growth relative to the maximum doubling time, μ_m observed off Oregon is calculated by normalizing Eppley's equation by μ_m,

$$\frac{\mu}{\mu_m} = ab^{cT}$$

where a becomes 0.851 doublings day$^{-1}/\mu_m$. The temperature distribution is specified from observations (Section 3c).

The herbivore grazing function is the Ivlev (1945) equation as modified by Parsons *et al.* (1967),

$$\begin{aligned} R &= R_m\,[1 - e^{-\Lambda(P-P_t)}]; && P > P_t \\ &= 0 && ; P \leq P_t \end{aligned}$$

where R is the rate of ingestion (hr^{-1}); R_m is the maximum ingestion rate; Λ ($l/\mu g$ at N) is the Ivlev constant which modifies the rate of change of ingestion with phytoplankton concentration, P; and P_t is the threshold concentration of phytoplankton at which grazing begins. The values of R_m, Λ and P_t are species specific (Frost, 1974; Mullin *et al.*, 1975). The grazing rate as a function of phytoplankton concentration is plotted for *Calanus pacificus* in Figure 3, using values from Parsons *et al.* (1967).

The loss of nitrogen from the phytoplankton population by cell autolysis is represented by the linear loss term, $-\Xi P$, although the process is a complex function of physiological stress. This term is essential in properly modeling the phytoplankton dynamics in the aphotic zone of the water column.

b. The herbivore equation. In the model herbivores are advected and diffused in the same manner as passive phytoplankton and dissolved nutrients. Zooplankton

express the variation of light with time of day
n a surface buoy 13 km off Sand Lake, Oregon
1974). Light attenuation with depth in the ocean
mbert law. Self-shading of the phytoplankton is
e exponential in (4).

saturated and nutrients are not limiting, the rate
function of temperature (Winter *et al.*, 1975).
conditions the specific growth rate μ (doublings
e empirically derived equation,

$$\mu = ab^{cT}$$

b is the constant 1.066, c is $1°C^{-1}$, and T is

erience a suppression of the growth rate above
nperatures are usually less than this optimum in
rical relationship is adequate for modelling pur-
relative to the maximum doubling time, μ_m,
normalizing Eppley's equation by μ_m,

$$\frac{\mu}{\mu_m} = ab^{cT}$$

y^{-1}/μ_m. The temperature distribution is speci-

s the Ivlev (1945) equation as modified by

$$- e^{-\Lambda(P-P_t)}]; P > P_t$$
$$; P \leq P_t$$

; R_m is the maximum ingestion rate; Λ ($l/\mu g$
odifies the rate of change of ingestion with
P_t is the threshold concentration of phyto-
values of R_m, Λ and P_t are species specific
grazing rate as a function of phytoplankton
ificus in Figure 3, using values from Parsons

toplankton population by cell autolysis is
P, although the process is a complex func-
s essential in properly modeling the phyto-
the water column.

l herbivores are advected and diffused in
kton and dissolved nutrients. Zooplankton

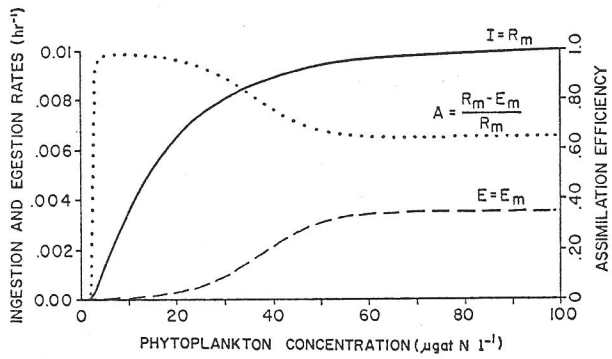

Figure 3. Ingestion and egestion rates and assimilation efficiency as functions of phytoplankton concentration. The solid line is ingestion rate, I, for *Calanus pacificus* where $R_m = 0.01$ hr^{-1}, $\Lambda = 0.06$ (μg at N/l)$^{-1}$ and $P_t = 2.5$ μg at N l^{-1}. The dashed curve is egestion rate, E, where $E_m = 3.5 \times 10^{-3}$ hr^{-1}, $\Delta = 2 \times 10^{-5}$ hr^{-1}, and $\Upsilon = 0.15$ (μg at N/l)$^{-1}$. The dotted curve is assimilation efficiency, A, calculated as $(I\text{-}E)/I$.

have the ability to change their position in the water column but their swimming capability cannot overcome horizontal advection. The collective physiology and behavior of the zooplankton over the Oregon continental shelf define the herbivore dynamics in this model. Since zooplankton species over the shelf exhibit little diel vertical migration (Peterson, 1972), this behavior is not simulated.

The biological terms in the zooplankton equation are written

$$\frac{\partial Z}{\partial t} = R_m [1 - e^{-\Lambda(P-P_t)}] Z - \frac{E_m \Delta e^{\Upsilon(P-P_t)} Z}{E_m + \Delta[e^{\Upsilon(P-P_t)}-1]} - \Gamma Z \qquad (5)$$

The first term on the right-hand side of (5) describes ingestion of phytoplankton by zooplankton; the second term formulates egestion of fecal pellets by zooplankton; and the third term represents metabolic excretion by zooplankton. Reproduction or natural death is not dealt with on the short time scale of concern here (days to weeks), although the herbivores can increase in biomass by assimilation of phytoplankton nitrogen.

Ingestion is calculated from the Ivlev equation discussed above. Egestion rate as a function of food availability (Fig. 3) is computed from the proposed expression

$$E = \frac{E_m \Delta e^{\Upsilon(P-P_t)}}{E_m + \Delta[e^{\Upsilon(P-P_t)}-1]}$$

where E_m (hr^{-1}) is the maximum egestion rate; Δ (hr^{-1}) is the egestion rate at the grazing threshold, P_t; and Υ (l/μg at N) determines the increase in egestion rate with increasing phytoplankton concentration, P. Conover (1966) suggests egestion is a constant proportion of food ingested by *Calanus hyperboreus* feeding over a wide range of diatom food concentrations. At low phytoplankton concentrations, however, egestion may no longer be a linear function of ingestion.

Steele (1974) and Frost (1974) recognized that efficiency of assimilation defined as (ingestion-egestion)/ingestion may be high when food is scarce, and would possibly decrease as food concentration increases. In Figure 3 the assimilation efficiency is calculated for a range of phytoplankton concentrations. Above the grazing threshold, where the assimilation efficiency is zero by definition, the efficiency rapidly increases and then decreases to a minimum value.

Metabolic excretion of nitrogen varies with grazing activity, temperature and growth stage. Nevertheless, the excretion process is expressed as a linear function of zooplankton biomass, $-\Gamma Z$, where Γ is a constant.

c. The detritus equation. Detritus in this model consists of copepod fecal pellets and ruptured phytoplankton cells. Detritus is considered to be passively advected and diffused in the same manner as the plankton and dissolved nutrients.

The biological terms affecting the local change in detritus are written

$$\frac{\partial D}{\partial t} = \frac{E_m \Delta e^{\Upsilon(P-Pt)} Z}{E_m + \Delta[e^{\Upsilon(P-Pt)} - 1]} + \Xi P - \Phi D \tag{6}$$

The term for bacterial remineralization of detrital nitrogen into ammonia is $-\Phi D$.

d. The ammonia and nitrate equations. The nutrient equations include the source for uptake by phytoplankton and the sink for excretion of metabolites by herbivores and the remineralization of detritus. Both ammonia and nitrate are passively advected and diffused.

The biological dynamics for ammonia are written

$$\frac{\partial NH_4}{\partial t} = \Phi D + \Gamma Z - V_m \frac{NH_4 P}{k_u + NH_4} - \Omega NH_4 \tag{7}$$

and those for nitrate are written

$$\frac{\partial NO_3}{\partial t} = \Omega NH_4 - V_m \frac{NO_3 P}{k_u + NO_3} e^{-\Psi NH_4} . \tag{8}$$

Bacterial oxidation of ammonia into nitrite and subsequently into nitrate is expressed by the term ΩNH_4. During CUE, NO_2^- and NO_3^- were measured as total NO_3^-. Thus, the model does not consider the nitrite intermediate.

e. Scaling of the equations. The biological dynamics (3) and (5) –(8) contain explicitly the parameters V_m, k_u, Ψ, R_m, Λ, P_t, Ξ, E_m, Δ, Υ, Γ, Φ, and Ω, and implicitly the initial concentrations P, Z, D, NO_3 and NH_4. By scaling the equations the number of parameters can be reduced. One nondimensional solution is then equivalent to solving several dimensional cases. To transform back to dimensional units, one multiplies the nondimensional solution by the scaling parameters.

One can examine all biological processes relative to the doubling time of the phytoplankton. If time, t, is scaled by V_m, parameter $\tau = tV_m$, where τ is nondimensional time. Also let P, Z, D, NO_3 and NH_4 be scaled by N_t, the total concen-

ration of nitrogen (μg at N l^{-1}) in all biotic components in the upwelling region.

In nondimensional space, (3) and (5) – (8) become

$$\frac{\partial P'}{\partial \tau} = f(I,T)\left(\frac{NO_3'}{\alpha + NO_3'} e^{-\psi NH_4'} + \frac{NH_4'}{\alpha + NH_4'}\right) P' - \beta(1 - e^{-\lambda(P'-P^*)})Z' - \xi P' \tag{9}$$

$$\frac{\partial Z'}{\partial \tau} = \beta\,(1 - e^{-\lambda(P'-P^*)})\,Z' - \frac{\rho\delta e^{\nu(P'-P^*)}\,Z'}{\rho+\delta[e^{\nu(P'-P^*)} - 1]} - \gamma Z' \tag{10}$$

$$\frac{\partial D'}{\partial \tau} = \frac{\rho\delta e^{\nu(P'-P^*)}\,Z'}{\rho+\delta[e^{\nu(P'-P^*)} - 1]} + \xi P' - \phi D' \tag{11}$$

$$\frac{\partial NH_4'}{\partial \tau} = \phi D + \gamma Z' - \frac{NH_4'P'}{\alpha+NH_4'} - \omega NH_4' \tag{12}$$

$$\text{and } \frac{\partial NO_3'}{\partial \tau} = \omega NH_4' - \frac{NO_3'P'}{\alpha+NO_3'} e^{-\psi NH_4'} . \tag{13}$$

The scaling relationships are listed in the Appendix. Note the units of $f(I, T)$ cancel. All quantities in (9)-(13) are nondimensional. P', Z', D', NO_3' and NH_4' are all fractions; if multiplied by 100 they represent the percent of N_t in that biotic component at time τ (i.e., a standing crop).

If the physical dynamics in (2) are also scaled, one can compare the relative influence of the physical and biological processes in determining the distribution of phytoplankton. Let

$$x = Lx' \qquad u = Uu'$$

$$z = Hz' \qquad w = Ww'$$

where L and H are characteristic horizontal and vertical length scales respectively. U is a typical value of the organized horizontal flow, and W is a typical value of the vertical velocity. Using the scaling relations put forth above, (2) becomes nondimensional,

$$\frac{\partial P'}{\partial \tau} + \left[\frac{U}{LV_m}\right] u' \frac{\partial P'}{\partial x'} + \left[\frac{W}{HV_m}\right] w' \frac{\partial P'}{\partial z'} - \left[\frac{K_h}{L^2V_m}\right]\frac{\partial^2 P'}{\partial x'^2}$$

$$- \left[\frac{K_v}{H^2V_m}\right]\frac{\partial^2 P'}{\partial z'^2} = \text{scaled biological dynamics.} \tag{14}$$

The scaling of the equations for herbivores, ammonia and nitrate is similar.

Detritus is assumed to have a constant sinking rate, w_s. The nutrients, NO_3' and NH_4', and the plankton, P' and Z', are assumed totally passive (i.e., $w_s = 0$). The detritus sinking rate is scaled in the same manner as the vertical velocity, w,

$$w_s = Ww_s'.$$

The total derivative for detritus may then be expressed as,

$$\frac{\partial D'}{\partial \tau} + S_1 u' \frac{\partial D'}{\partial x'} + S_2 (w' + w_s') \frac{\partial D'}{\partial z'} - E_h \frac{\partial^2 D'}{\partial x'^2} - E_v \frac{\partial^2 D'}{\partial z'^2} = \text{scaled biological dynamics} \quad (15)$$

where $S_1 = U/(LV_m)$, $S_2 = W/(HV_m)$, $E_h = K_h/(L^2V_m)$, and $E_v = K_v/(H^2V_m)$. Hereafter the primes are dropped for convenience.

f. Estimation of the model parameter values. Upon formulating this time dependent, spatial, marine plankton model, one must next determine the proper parameter values for application of these equations to the Oregon upwelling ecosystem.

The highest temperature observed within 50 km of the Oregon coast during strong upwelling in August 1973 was 14°C. At this temperature the maximum growth rate of the phytoplankton is expected to be 2.08 doublings day^{-1} (Eppley, 1972), provided light and nutrients are not limiting. Thus, $V_m = 0.08$ hr^{-1}.

A typical value of the half-saturation constant, k_u, for neritic diatoms in upwelling areas is 1 μg at N l^{-1} for both nitrate and ammonia (Eppley *et al.*, 1969; MacIsaac and Dugdale, 1969). Newly upwelled waters off Oregon have a maximum total nitrogen concentration (N_t) of approximately 30 μg at N l^{-1}. Upon scaling by N_t, the nondimensional half-saturation parameter, α, is 0.03. Parameter α typically ranges from 10^{-1} to 10^{-2} for most oceanic areas (O'Brien and Wroblewski, 1976). Lower values of α correspond to phytoplankton utilizing extremely small concentrations of the limiting nutrient.

The exponential reduction in V_m (NO_3) as a function of NH_4 concentration is best described using $\Psi = 1.462$ (μg at $NH_4/l)^{-1}$ (Fig. 1). Upon scaling by N_t, nondimensional $\psi = 43.86$.

The P_h vs. I curve modified from Vollenweider (1965) can reproduce the laboratory response of diatom growth to light intensity (Ryther, 1956) if $I_s = 0.07$ cal cm^{-2} min^{-1}, $\theta = 0.175$ and $\eta = 4.3$. Solar radiation measurements made off the Oregon coast in August, 1973, indicate a value for I_m of 1.25 cal cm^{-2} min^{-1} on a cloudless day, and a twilight to twilight period of 13 hours (Reed and Halpern, 1974). A daylength, d, of 12 hours has been assumed in the model for simplicity.

In coastal waters incident radiation is reduced by a factor of two within the first few centimeters of the water column as ultraviolet and infrared radiation is absorbed (Parsons and Takahashi, 1973); thus the factor, 0.5, appears in (4). Small and Curl (1968) determined a value for κ_w of 0.067 m^{-1} off Oregon. The value is higher than expected for the absorption of light by pure seawater (0.040 m^{-1}) due to non-chlorophyllous, colored, dissolved substances from the Columbia River discharge. Using the data presented in Small and Curl (1968) and assuming a chlorophyll **a**/N ratio of 1/8 (Anita *et al.*, 1963), a value for κ_p of 0.095 cm^2 (μg at N)$^{-1}$ is estimated for the Oregon upwelling season.

One can approximate the loss rate of phytoplankton nitrogen below the euphotic zone in terms of the plant population's e-folding rate. The time scale Ξ^{-1} is the time

$w_s') \frac{\partial D'}{\partial z'} - E_h \frac{\partial^2 D'}{\partial x'^2} - E_v \frac{\partial^2 D'}{\partial z'^2} =$

biological dynamics (15)

$_n)$, $E_h = K_h/(L^2 V_m)$, and $E_v = K_v/(H^2 V_m)$.

onvenience.

alues. Upon formulating this time dependent, must next determine the proper parameter s to the Oregon upwelling ecosystem.

within 50 km of the Oregon coast during 14°C. At this temperature the maximum pected to be 2.08 doublings day^{-1} (Eppley, not limiting. Thus, $V_m = 0.08$ hr^{-1}.

n constant, k_u, for neritic diatoms in upwell- nitrate and ammonia (Eppley *et al.*, 1969; pwelled waters off Oregon have a maximum proximately 30 μg at N l^{-1}. Upon scaling on parameter, α, is 0.03. Parameter α typi- st oceanic areas (O'Brien and Wroblewski, to phytoplankton utilizing extremely small

O_3) as a function of NH_4 concentration is t $NH_4/l)^{-1}$ (Fig. 1). Upon scaling by N_t,

enweider (1965) can reproduce the labora- intensity (Ryther, 1956) if $I_s = 0.07$ cal olar radiation measurements made off the a value for I_m of 1.25 cal cm^{-2} min^{-1} on t period of 13 hours (Reed and Halpern, een assumed in the model for simplicity. reduced by a factor of two within the first traviolet and infrared radiation is absorbed factor, 0.5, appears in (4). Small and Curl 67 m^{-1} off Oregon. The value is higher y pure seawater (0.040 m^{-1}) due to non- nces from the Columbia River discharge. Curl (1968) and assuming a chlorophyll value for κ_p of 0.095 cm^2 (μg at N)$^{-1}$ is

nytoplankton nitrogen below the euphotic lding rate. The time scale Ξ^{-1} is the time

necessary to reduce a light limited or nutrient starved population to approximately one third of its initial concentration, P_o. Under no growth conditions,

$$\frac{P}{P_o} = e^{-\Xi\tau} = e^{-1} \text{ when } \tau = \Xi^{-1}.$$

The exact determination of Ξ in nature is difficult. It is estimated the phytoplankton standing crop is reduced to $P_o e^{-1}$ in 10 days, so nondimensional $\xi = 0.05$.

For continuously grazing *Pseudocalanus* sp., a major herbivore over the Oregon shelf, $R_m = 0.02$ hr^{-1} (Parsons *et al.*, 1967). Upon scaling by V_m, nondimensional $\beta = 0.25$. The species-specific Ivlev constant is 0.06 (μg at N/l)$^{-1}$ and the grazing threshold is less than 2.5 μg at N l^{-1}. Upon scaling by N_t, nondimensional $\lambda = 1.8$ and $P^* < 0.08$. A value for P^* of zero is used in all the following model solutions to test the hypothesis that a positive grazing threshold is necessary for ecosystem stability (Steele, 1974).

The maximum egestion rate is chosen to simulate a minimum assimilation efficiency of 65% (Corner and Davies, 1971) under superfluous grazing conditions (i.e., $E_m = 35\%$ of R_m). Thus, nondimensional $\rho = 0.35\beta$. There is currently no published laboratory data on the values of egestion parameters Δ and Υ. Based on unpublished work by J. Hirota and deduction, Υ is chosen as 0.15 (μg at N/l)$^{-1}$ or nondimensional $\nu = 4.5$. For near complete assimilation of nitrogen at the grazing threshold, Δ is 7.2×10^{-4} hr^{-1} or $\delta = \Delta/V_m = 0.01$.

Calanus finmarchicus grazing on an algal diet in 10°C waters of the Clyde Sea was estimated by Corner *et al.* (1965) to excrete 8-11% of its body nitrogen per day. A value of 10% will be used in this model; therefore, nondimensional $\gamma = 0.10$.

Most of the detritus in the model originates from copepod fecal pellet production. Redfield *et al.* (1963) have suggested that much of the soluble nitrogen in newly formed fecal pellets dissolves before the particle sinks out of the euphotic zone. If it is assumed that 40% of the ammonia in fecal pellets leaches out in 1 day, then parameter $\phi = 0.5$.

The rate of oxidation of ammonia into successively nitrite and nitrate in the ocean is a function of temperature, pressure and bacterial activity (Von Brand and Rakestraw, 1940). From the data provided by Von Brand *et al.* (1937), an *e*-folding time for oxidation of ammonia to nitrite-nitrate appears to be about 25 days. Thus $\omega = 0.02$.

Scaling parameters L and H can be regarded as the length scales within which mesoscale structures in the plankton distributions occur. Phytoplankton plumes off Oregon are less than 50 km in horizontal length and 50 m in depth; thus $L = 50$ km and $H = 50$ m. The resolution of the structures is determined by the choice of Δx and Δz, which must be at least several times smaller than these scales. A value for K_h of 5×10^5 cm^2 sec^{-1} is chosen based on the length scale, L (Okubo, 1971).

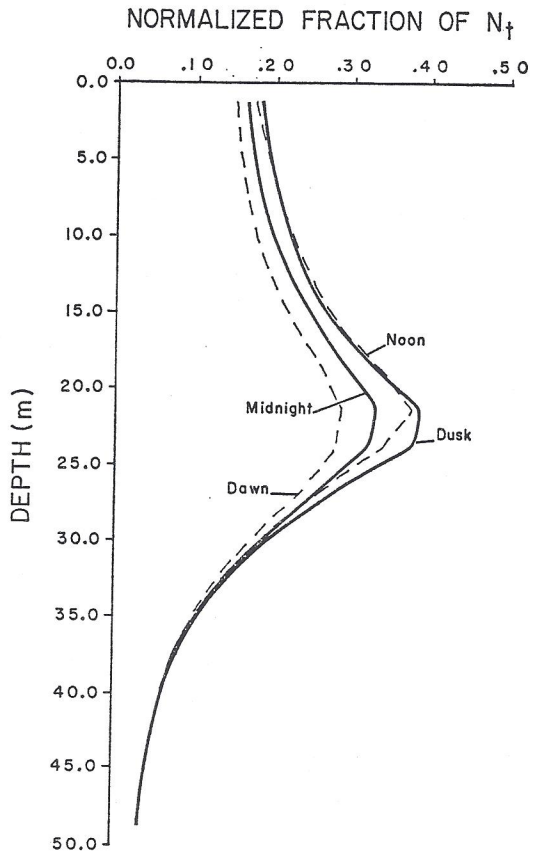

Figure 4. Steady state oscillation in the phytoplankton profile of the (z,t) model. Plant biomass is expressed as a nondimensional fraction of the total concentration of nitrogen in the upwelling ecosystem, N_t.

Experiments conducted off Oregon by Halpern (1974) suggest a value for K_v of 1 cm^2 sec^{-1}. Higher values for K_v are observed over short time scales (Halpern, 1974; Kullenberg, 1976). In this model K_v is chosen such that the role of vertical diffusion is approximately the same as horizontal diffusion on the smallest resolvable length scales, i.e., $K_v = K_h\,(\Delta z/\Delta x)^2 \approx 1$ cm sec^{-1}.

Explicit modeling of the upwelling circulation (Section 3) yields characteristic values of the horizontal and vertical velocities, U and W, of 10 cm sec^{-1} and 2×10^{-2} cm sec^{-1} respectively.

The nondimensional coefficients in (14) define the importance of the advective terms relative to the diffusive and biological terms in the equation. When $U/(LV_m)$ or $W/(HV_m) >> 1$, advection plays a dominant role in determining the spatial configuration of the phytoplankton biomass (O'Brien and Wroblewski, 1973). If one

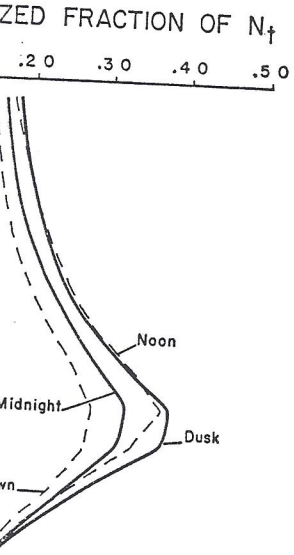

plankton profile of the (z,t) model. Plant bio-
n of the total concentration of nitrogen in the

pern (1974) suggest a value for K_v of 1
ed over short time scales (Halpern, 1974;
osen such that the role of vertical diffu-
ital diffusion on the smallest resolvable
sec^{-1}.
ulation (Section 3) yields characteristic
ies, U and W, of 10 cm sec^{-1} and 2 ×

define the importance of the advective
terms in the equation. When $U/(LV_m)$
nant role in determining the spatial con-
'Brien and Wroblewski, 1973). If one

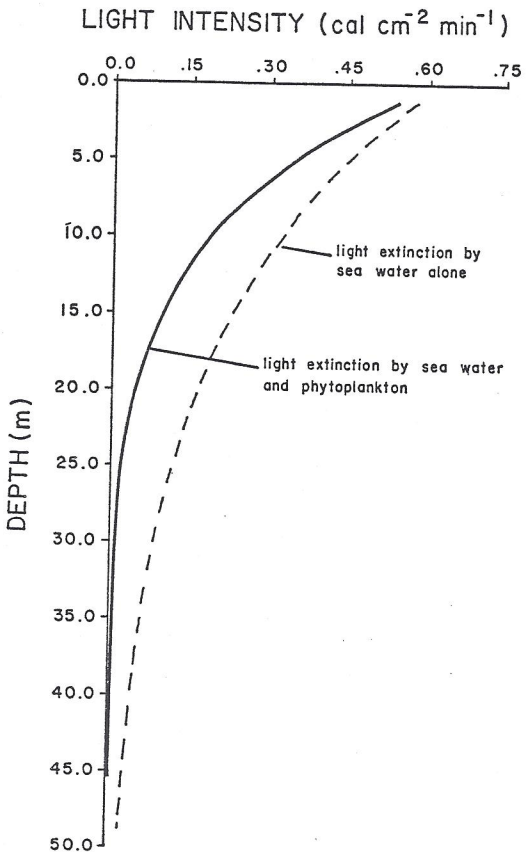

Figure 5. Light intensity-depth profile at midday in the steady state solution of the (z,t) model.

evaluates the magnitude of these coefficients using the values presented above, it is evident that vertical advection is twice as important as horizontal transport in determining the distribution of the phytoplankton. The diffusion terms are two orders of magnitude smaller than the advective terms. The advective terms and the biological terms are the same order of magnitude.

g. Steady state solution of the (z,t) model. The ability of the above formulations to simulate nitrogen distribution in a neritic water column off Oregon is tested by comparing model solutions to observations. The scaled equations for P, Z, NO_3, NH_4, and D are solved neglecting all advective terms and horizontal dependence. The (z,t) model does include diffusion of the dependent variables in the vertical and light extinction with depth. A temperature profile corresponding to that specified for a water column 50 km offshore (Section 3c) is assumed.

Figure 4 displays the steady state, vertical phytoplankton profiles which result.

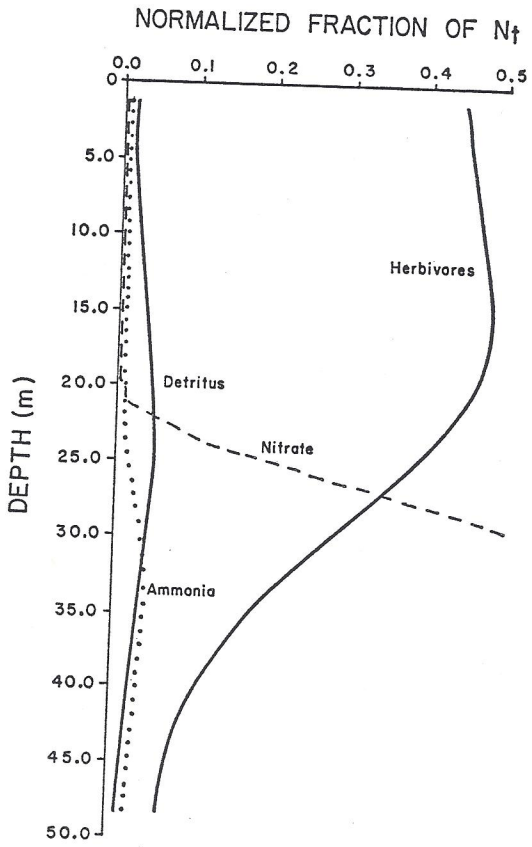

Figure 6. Steady state herbivore, detritus, nitrate and ammonia profiles of the (z,t) model at midday. The dependent variables are expressed as nondimensional fractions of N_t.

The profiles fluctuate as incident radiation follows the sine curve and photosynthetically active light penetrating the surface is attenuated with depth. A phytoplankton maximum occurs at a depth of 20 to 25 m. Sampling profiles taken 50 km offshore during CUE often showed a chlorophyll maximum between 10 and 25 m.

Figure 5 shows the light intensity-depth profile at midday. If light absorption by phytoplankton were not considered (i.e., if $\kappa_p = 0$), the 1% I_o light intensity would reach 68 m instead of 33 m. Light intensities greater than 0.13 cal $cm^{-2}min^{-1}$ suppress phytoplankton growth in the upper 15 m (Fig. 4). Photoinhibition has been observed at offshore stations to depths of 15 m at local noon during summer (L. Small, unpublished data).

The zooplankton, detritus, nitrate and ammonia profiles at midday are shown in Figure 6. Oscillations occur in the nitrate and ammonia profiles but are not depicted. Nutrient depletion is evident in the upper 21 meters of the water column, both nitrate and ammonia increasing in concentration below this depth as phyto-

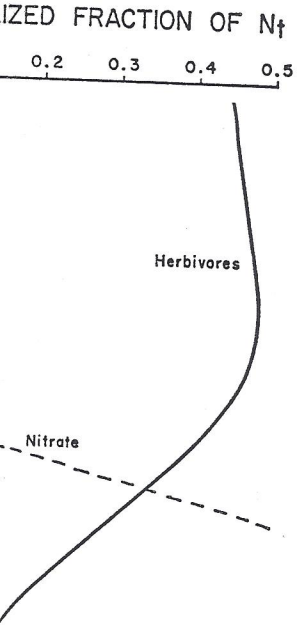

rate and ammonia profiles of the (z,t) model at
ed as nondimensional fractions of N_t.

n follows the sine curve and photosynthetic
is attenuated with depth. A phytoplankton
m. Sampling profiles taken 50 km offshore
naximum between 10 and 25 m.
h profile at midday. If light absorption by
if $\kappa_p = 0$), the 1% I_o light intensity would
nsities greater than 0.13 cal $cm^{-2}min^{-1}$
pper 15 m (Fig. 4). Photoinhibition has
ths of 15 m at local noon during summer

ammonia profiles at midday are shown in
e and ammonia profiles but are not de-
ie upper 21 meters of the water column,
concentration below this depth as phyto-

plankton growth becomes light limited. The herbivore standing stock is highest in the euphotic zone. Zooplankton biomass is directly related to the concentration of its prey through the Ivlev grazing term. If zooplankton were not diffused in the vertical (i.e., if $K_v = 0$) the profile would more closely follow the phytoplankton profile and would show a lower herbivore concentration near the surface. Detritus, which in these solutions is assumed to sink at a rate of 8 m day^{-1}, shows a maximum at 25 m. If a sinking rate of zero were assumed, the shape of the detritus profile would more closely follow the zooplankton profile, since egestion of fecal pellets is the main source of detritus. Detritus sinking at a rate of 100 m day^{-1} (Smayda, 1969) would have a profile of uniformly low concentration, prohibiting an ammonia maximum from forming in the modeled upper 50 m of the water column.

The steady state P, NO_3 and NH_4 profiles shown in Figures 4 and 6 approximate the observed profiles of chlorophyll, nitrate and ammonia taken 50 km seaward of the Oregon coast in August, 1973, (not shown). Continuous profiles of zooplankton biomass and detrital nitrogen were not taken at this station, but zooplankton net tows and the particulate nitrogen data do indicate the (z,t) model's solutions are reasonable.

h. Calculations of daily gross primary production. Given the phytoplankton vertical distribution, the rate, V, at which inorganic nitrogen is incorporated into phytoplankton nitrogen, P, can be calculated. Integration of the growth of phytoplankton over depth, $\int_z VP$, where V is a function of light, temperature and nutrients gives the gross primary productivity (mg N m^{-2} hr^{-1}) of the water column.

In the (z, t) model, daily gross primary production is found by integrating (3) over depth for a 24 hour period, while neglecting the loss terms for herbivore grazing and phytoplankton autolysis. The water column in Figure 4 has a daily gross production of 100 mg N m^{-2}.

Anderson (1964) observed a range of daily net primary production from 0.3 to 1.2 g C m^{-2} day^{-1} in oceanic waters off Oregon during the summer of 1962. Assuming a C/N ratio of 7 (Small and Ramberg, 1971), this production in terms of nitrogen is 43 to 171 mg N m^{-2} day^{-1}. It appears the biological dynamics formulated in this section can correctly simulate primary production off Oregon.

3. Model formulation—the physical dynamics

Biological processes can interact with physical transport mechanisms to create mesoscale features in the plankton and nutrient fields called plumes and tongues.[4]

4. The ICSU Scientific Committee on Ocean Research (SCOR) Working Group 36 during their 1974 meeting in Kiel, Germany recommended use of the term "tongue" to refer to features in the distribution of biological and chemical variables which have a predominant horizontal length scale, such as a shallow coastal bloom of phytoplankton. "Plumes" should refer to coastal blooms with a significant vertical extension.

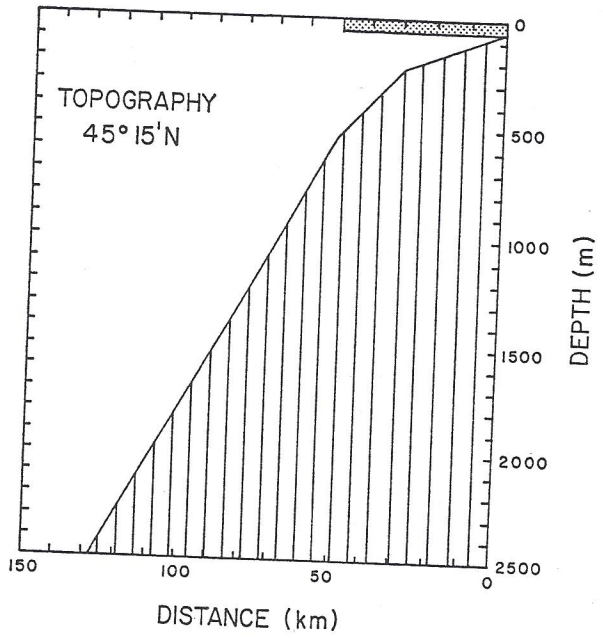

Figure 7. Bottom topography assumed in the zonal, upwelling circulation model of Thompson (1974). The rectangular stippled region at the upper right delineates the region of the ecosystem model.

An often observed length scale of phytoplankton patchiness in coastal upwelling areas is 5 to 10 km (Beers *et al.*, 1971; Walsh *et al.*, 1974; Kelley *et al.*, 1975). To resolve the formation and dissipation of plumes and tongues, the upwelling circulation must be known to great detail.

Thompson (1974) developed an (x,z,t) numerical model of the zonal circulation off Oregon which simulates the response of the ocean to a coastal wind stress. The circulation model forecasts a time dependent velocity field which was used to advect the dependent variables P, Z, NO_3, NH_4 and D. The physical dynamics incorporate the effects of bottom topography, a time dependent wind stress, incident solar radiation, and surface, interfacial, and bottom stresses. The prediction of vertical mixing is based on a parameterization of boundary and shear generated turbulence. The model delineates the position of the seasonal pycnocline and the localities of upwelling, convergences and divergences.

The upwelling model was run under two different wind stress forcings: 1) a theoretical, steady wind stress favorable for upwelling; and 2) a wind stress calculated from anemometer data recorded at Newport, Oregon. The bottom topography incorporated in the model is a linearized version of the actual bottom slope off Oregon (Fig. 7). A bottom depth of 50 m at the coast is assumed to simplify computations.

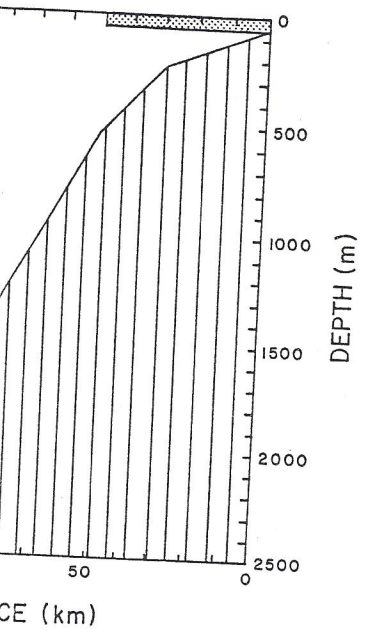

he zonal, upwelling circulation model of Thompson
at the upper right delineates the region of the eco-

ytoplankton patchiness in coastal upwelling
; Walsh *et al.*, 1974; Kelley *et al.*, 1975). To
f plumes and tongues, the upwelling circula-

z,t) numerical model of the zonal circulation
se of the ocean to a coastal wind stress. The
endent velocity field which was used to ad-
O_3, NH_4 and *D*. The physical dynamics in-
phy, a time dependent wind stress, incident
l, and bottom stresses. The prediction of
erization of boundary and shear generated
osition of the seasonal pycnocline and the
divergences.

wo different wind stress forcings: 1) a theo-
upwelling; and 2) a wind stress calculated
yport, Oregon. The bottom topography in-
rsion of the actual bottom slope off Oregon
coast is assumed to simplify computations.

A basic assumption of both the circulation and ecosystem models is no longshore variation in the coastline, bottom topography or velocity field. This simplifies the dynamics to a degree that fundamental features in the circulation and in the nitrogen distribution can be examined without the complexity imposed by longshore variability. Longshore variation in upwelling has been discussed by Shaffer (1974) and modeled by Hurlburt (1974) and Peffley and O'Brien (1976). However, consideration of longshore derivatives in (1) is left to future, more ambitious undertakings.

a. Numerical methods. Although the ocean basin of the circulation model is 3100 km wide (Thompson, 1974), all biological simulations are confined to the upper 50 m of the water column in a region within 50 km of the coast (Fig. 7). This area is divided into a grid with spacings at 2.5 m in z and 1 km in x. The first grid point is 1.25 m below the sea surface. The scaled equations for P, Z, NO_3, NH_4 and D are expressed in finite difference form and solved numerically for each grid point.

A detailed description of the numerical methods used in the ecosystem model can be found in Wroblewski (1976). In essence, the differencing of the equations incorporates a leap-frog scheme in time, a quadratic-conservative, advective scheme suggested by Piacsek and Williams (1970), and an explicit scheme for the diffusive terms. The diffusive and biological terms are lagged in time. The accuracy of the finite differencing scheme in approximating its analogous continuous derivatives increases with smaller time steps. The value of $\Delta\tau$ used was 0.02, which converts to 0.01 days in real time.

b. Boundary conditions. No advective mass flux is allowed across the coastal boundary or the air-sea interface. At the bottom water column boundary, the direction of the flow determines the advective boundary condition. If water is downwelling, the concentration of the variable just inside the boundary determines the value at the boundary. If water is upwelling, the boundary values for P, Z, NO_3, NH_4 and D must be specified. The steady state value of the variable at 50 m in the (z,t) model is taken as the concentration in water entering the model region from below.

The offshore boundary is treated similarly. The steady state profiles in Figures 4 and 6 specify the advective boundary conditions for water horizontally transported into the model region. No diffusive mass flux is allowed through any boundary.

These boundary conditions are such that limiting nutrient can become stored within the model region as either P, Z, NO_3, NH_4 or D, yet the total amount of nutrient is conserved in a balance between what is advected into and out of the region, and what is stored as standing stock or dissolved nutrient.

c. Initial conditions. Adequate field data does not exist to specify the initial conditions of the biological dependent variables for all x and z at the onset of the model case runs. Therefore, the initial conditions are taken as the steady state solution of the (x,z,t) ecosystem model in the absence of advection.

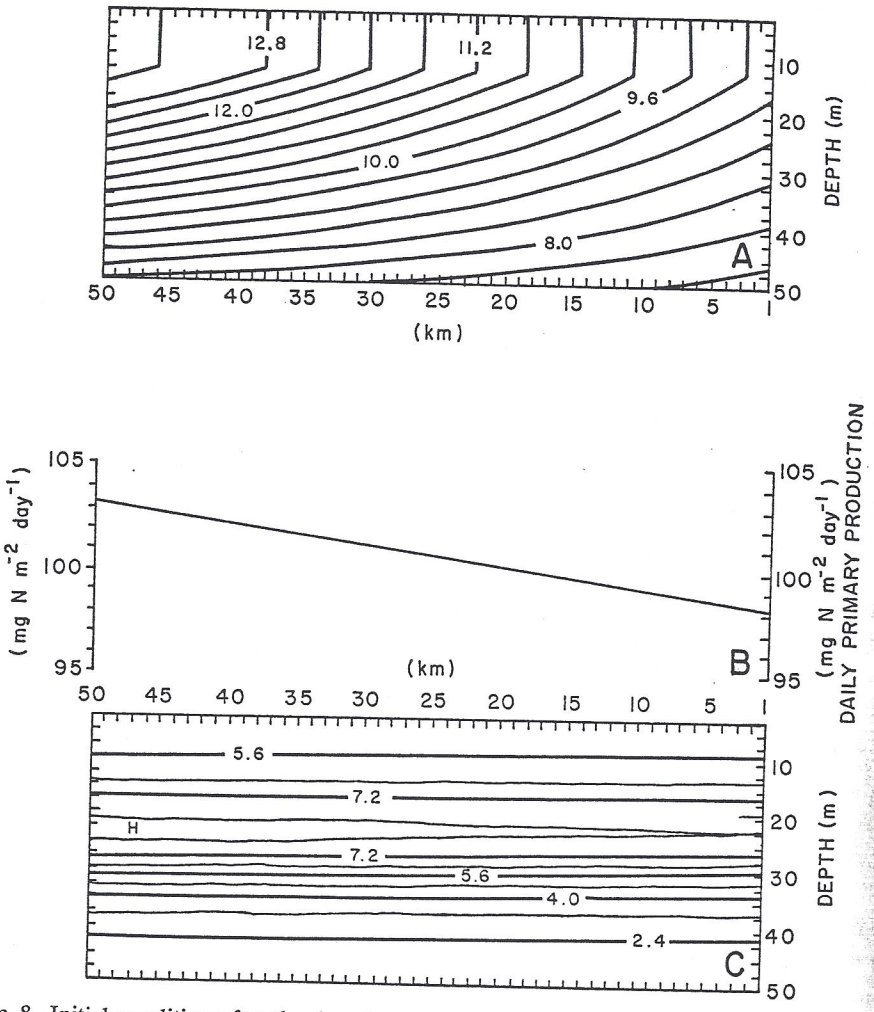

Figure 8. Initial conditions for the (x,z,t) ecosystem model: (a) The distribution of seawater temperature. Contours are from 7°C at 50 m depth at the coast to 14°C at the surface, 50 km offshore. The contour interval is 0.4°C. (b) The steady state, daily gross primary production. (c) The steady state phytoplankton distribution in the absence of advection. Contour intervals are 0.8 μg at N l^{-1}.

The temperature field incorporated in the model is specified from observations. Sea surface temperatures during strong upwelling in August 1973 were found to decrease from 14°C at an offshore distance of 50 km to 9°C at the coast. Temperature below the surface mixed layer decreased rapidly with depth. A polynomial function was fit to the observed temperature data to give a time invariant, smoothed temperature field evaluated at each grid point in the model region (Fig. 8a).

The influence of this temperature distribution on the steady state, daily gross

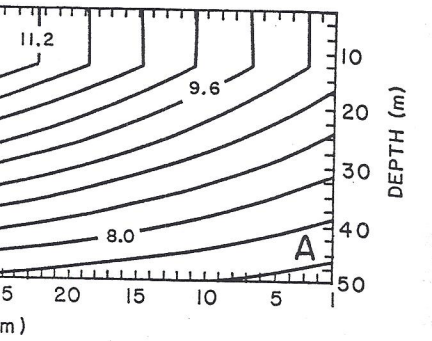

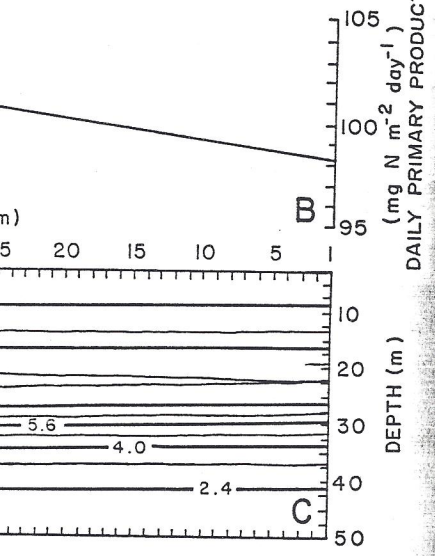

stem model: (a) The distribution of seawater n depth at the coast to 14°C at the surface, °C. (b) The steady state, daily gross primary distribution in the absence of advection. Con-

he model is specified from observations. owelling in August 1973 were found to of 50 km to 9°C at the coast. Tempera- ased rapidly with depth. A polynomial e data to give a time invariant, smoothed int in the model region (Fig. 8a).

ibution on the steady state, daily gross

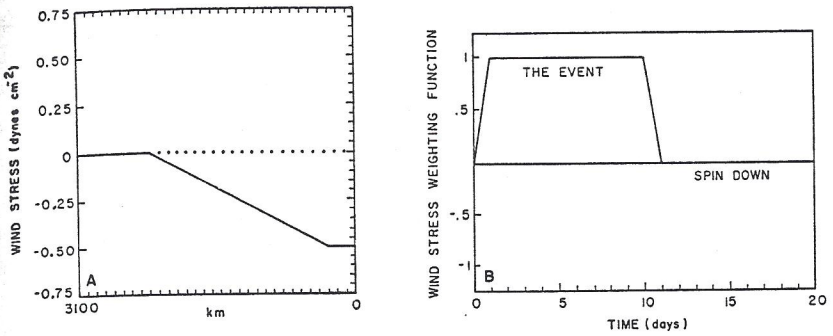

Figure 9. The north-south component of the wind stress in the strong upwelling case. (a) The distribution of the wind stress over the circulation model's ocean basin. (b) The temporal variation of the wind stress weighting function.

primary production of the water column is shown in Figure 8b. Figure 8c displays the corresponding phytoplankton field. The phytoplankton distribution is no longer homogeneous in x, as plant growth now varies with the horizontal temperature gradient.

In what will henceforth be referred to as the "strong upwelling case," a spatially variable wind stress is specified which linearly increases from zero at time zero to -0.5 dyne cm^{-2} (Fig. 9a and b). The wind stress remains at this magnitude from day 1 to day 10, then linearly decreases to zero during day 11. It remains zero for the rest of the modeled 20-day period. The east-west component of the wind stress is always zero.

A second wind stress which is more variable in time was used in the "intermittent upwelling case" (Section 4d). This model run is so named because the rate of upwelling predicted by the circulation model fluctuates with change in the magnitude of the wind stress. The dimensional parameter values used in both the strong and intermittent upwelling cases are recounted in Table 1.

4. Model results

a. The onset of strong upwelling and development of a phytoplankton plume. It is difficult to represent graphically the time dependent nature of the velocity field and the corresponding spatial features of the biological dependent variables. The following "snapshot" displays of these fields do not show the diel periodicity which occurs, for example, in phytoplankton growth or in the concentration of ammonia and nitrate. As a convention, the velocity field and the corresponding distribution of the dependent variables are displayed at the end of a model day. The nondimensional model solutions have been multiplied by N_t to regain units of concentration.

The velocity field after 4 days elapsed time in the strong upwelling case is pre-

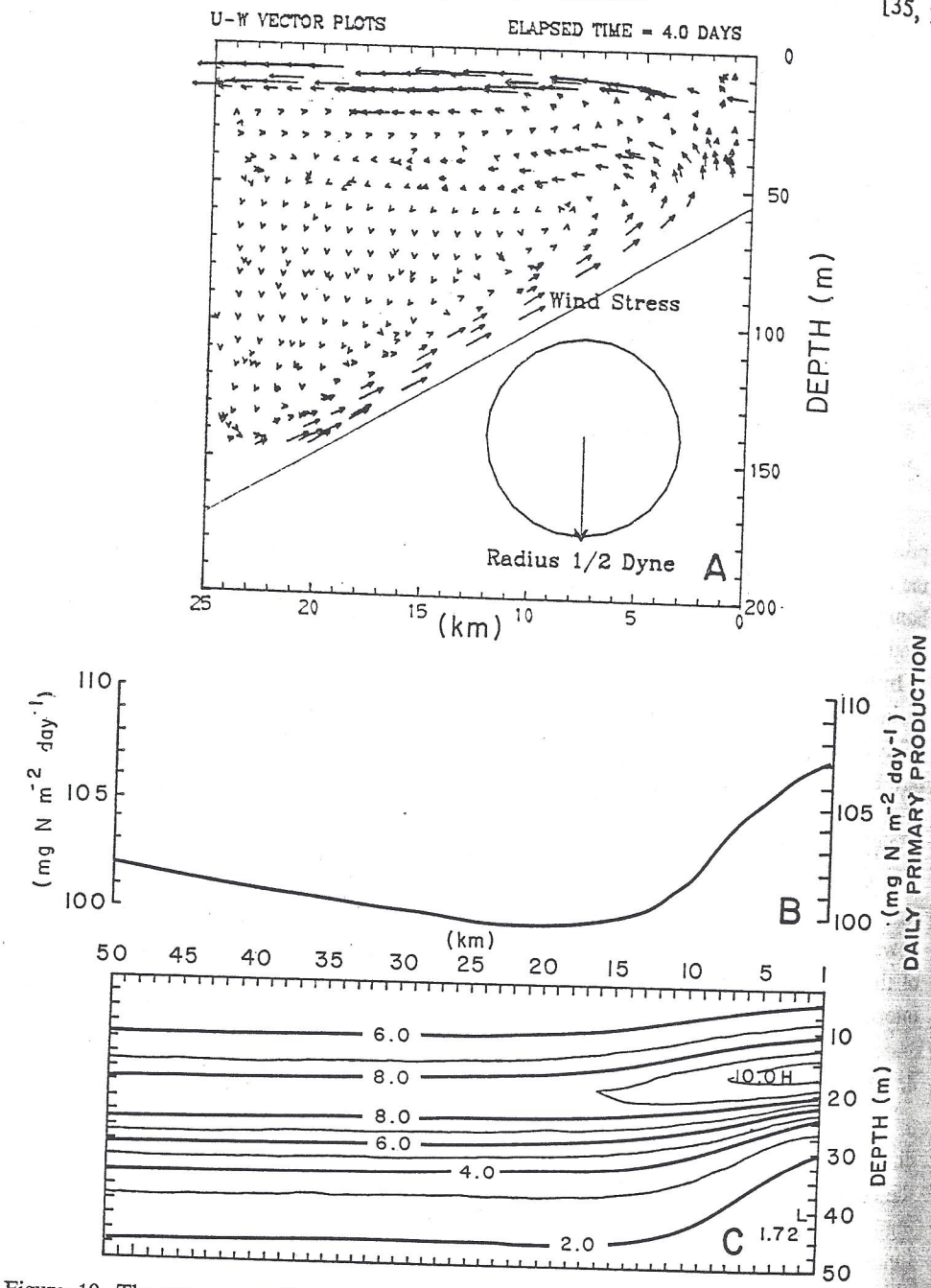

Figure 10. The strong upwelling case, after 4 days elapsed time: (a) The circulation in the transverse plane normal to the coast, the bottom topography, and the wind stress. The maximum u and w velocities in the field are -2.9 cm sec^{-1} and 1.4×10^{-2} cm sec^{-1}, respectively. (b) The daily gross primary production of the water column. (c) The distribution of phytoplankton. Contour intervals are 1 μg at N l^{-1}.

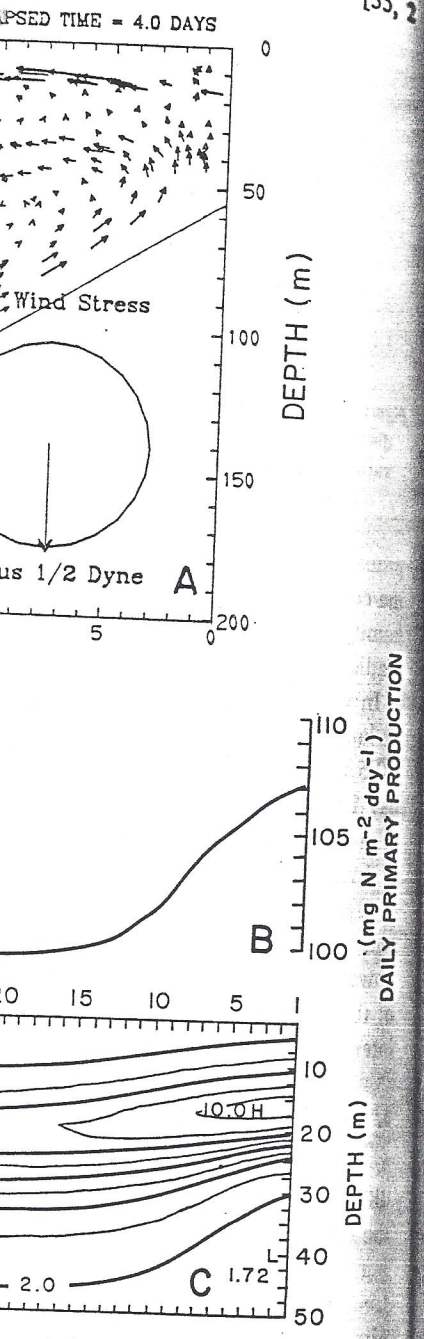

apsed time: (a) The circulation in the graphy, and the wind stress. The maxi- and 1.4×10^{-2} cm sec^{-1}, respectively. column. (c) The distribution of phyto-

sented in Figure 10a. The wind stress vector at the time of the velocity field snapshot has a magnitude of -0.5 dyne cm^{-2} and points southward. The velocity field is visualized by vectors representing the position and instantaneous velocity of tracer particles which have been advected by the flow. Only the vectors within 25 km of the coast are shown. The vector arrows are scaled by the maximum vector occurring in the field at that time. Each vector's horizontal and vertical scales differ by two orders of magnitude.

Two cyclonically rotating circulation cells are evident in Figure 10a. The lower cell advects water toward the coast along the sloping bottom and up into the euphotic zone. This upwelled water either continues to rise to the surface or moves offshore beneath the second counterclockwise rotating circulation cell. In this second cell the flow is weakly onshore at 30 m depth and strongly offshore near the surface. This two-cell circulation is similar to the conceptual diagram of coastal upwelling off Oregon presented by Mooers, Collins, and Smith (1976).

The daily gross primary production of the water column (Fig. 10b) is plotted above the corresponding phytoplankton field for day 4 (Fig. 10c). These figures show that as upwelling supplies nitrate to the nutrient-limited euphotic zone, primary productivity increases. The plants grow fastest where the supply of nutrients is greatest, in spite of the colder temperature near the coast (Fig. 8a). Figure 10c shows formation of a phytoplankton plume begins near the coast with the onset of upwelling.

After 7 days the two-cell circulation (Fig. 11a) and the phytoplankton plume (Fig. 11c) are well developed. A maximum plant biomass occurs at 17 m depth between 6 and 11 km offshore. The origin of this phytoplankton nitrogen is near the coast where primary productivity is highest (Fig. 11b). The plants are then advected away from the coast by the strong surface Ekman transport (Fig. 11a).

By day 10 downwelling develops in the region between 6 and 20 km offshore (Fig. 12a). Contours of the phytoplankton, zooplankton and nitrate fields clearly show the downwelling (Fig. 12c, 13a and b). The phytoplankton maximum increases as it is advected further offshore (Fig. 12c). Primary production increases not only at the locus of upwelling, but also in the surface waters which are advected seaward (Fig. 12b).

The zooplankton field at day 10 (Fig. 13a) depicts the upwelling and seaward transport of water low in herbivore biomass. The highest zooplankton concentrations occur seaward of the phytoplankton plume. The concentration of nitrate in the euphotic zone (Fig. 13b) is kept low by plant production. Only where strong upwelling occurs does the supply of NO_3 exceed its utilization, allowing high concentrations of nitrate to reach the surface.

During the first 10 days of the strong upwelling case, a detritus plume (Fig. 14a) develops several meters below and several kilometers seaward of the phytoplankton plume. Herbivores grazing in the phytoplankton plume produce fecal pellets which

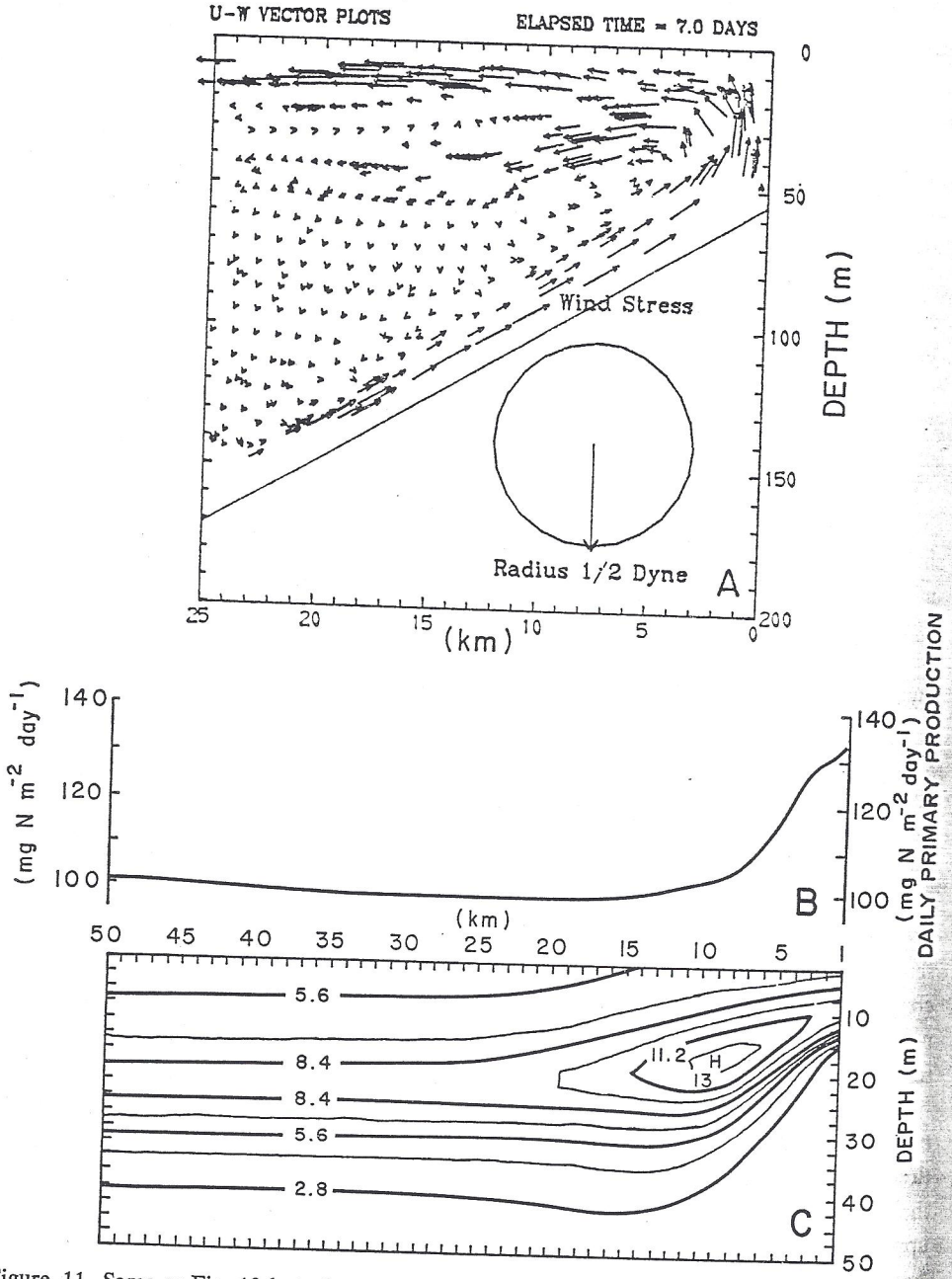

Figure 11. Same as Fig. 10 but after 7 days. The maximum u and w velocities in (a) are -5.9 cm sec^{-1} and 4.4×10^{-2} cm sec^{-1}, respectively. Contour intervals in (c) are 1.4 μg at N l^{-1}.

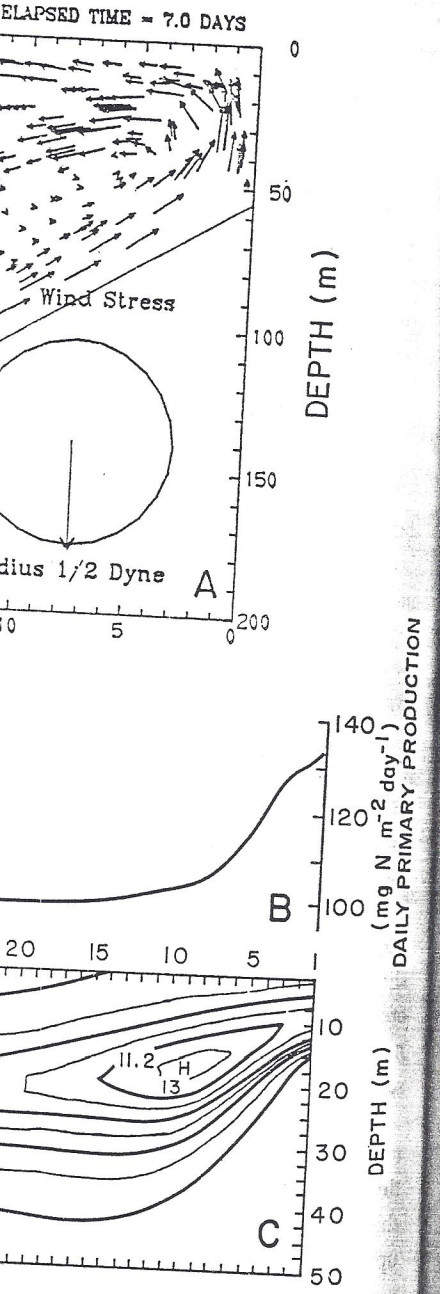

mum u and w velocities in (a) are -5.9
our intervals in (c) are 1.4 μg at N l^{-1}.

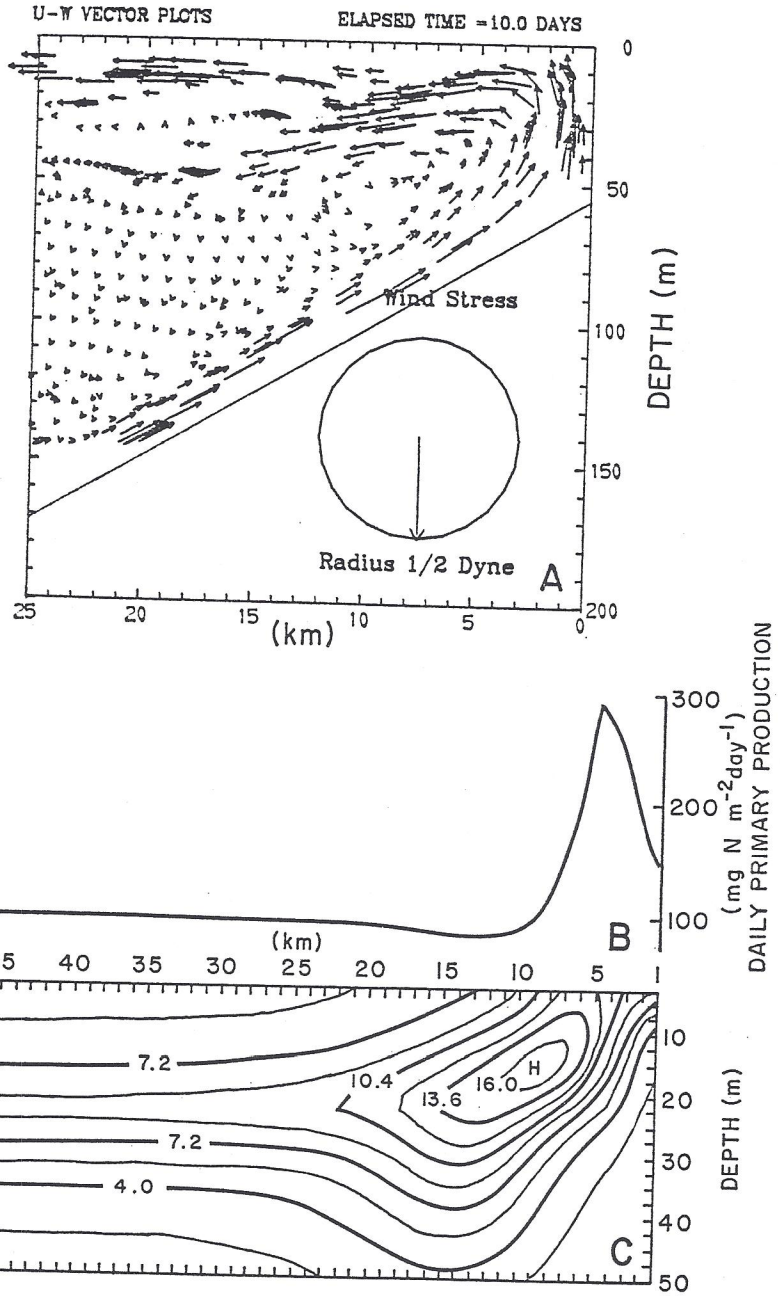

Figure 12. Same as Fig. 10 but after 10 days. The maximum u and w velocities in (a) are -6.1 cm sec^{-1} and 5.2×10^{-2} cm sec^{-1}, respectively. Contour intervals in (c) are 1.6 μg at N l^{-1}.

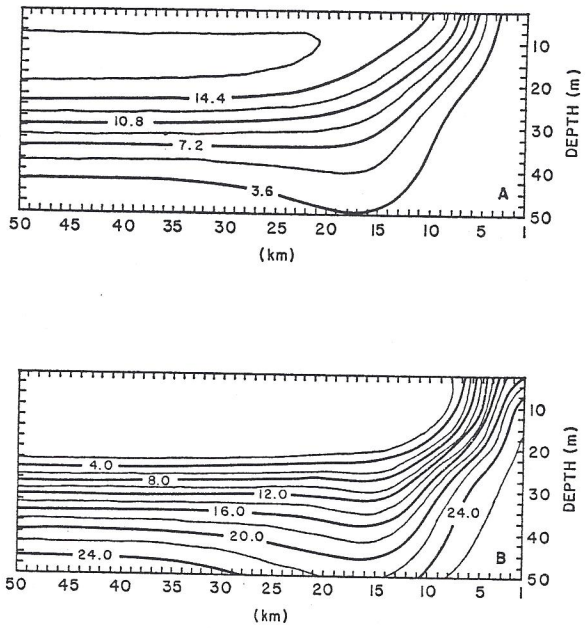

Figure 13. The strong upwelling case, after 10 days: (a) The zooplankton field. Contour intervals are 1.8 μg at N l^{-1}. (b) The nitrate field. Contour intervals are 2 μg at NO_3 l^{-1}.

sink as they are advected offshore. At day 10 an ammonia maximum exists at a depth of 40 m between 25 and 33 km offshore (Fig. 14b). The ammonia input from decomposing fecal pellets has exceeded the slower oxidation of ammonia into nitrate, resulting in high concentrations of NH_4 in this region.

b. Cessation of upwelling and decay of the phytoplankton plume. As the wind stress falls to zero during day 11 (Fig. 9b), both the coastal upwelling and the offshore downwelling begin to relax. The phytoplankton in the newly upwelled water remain longer in the euphotic zone. The highest plant concentration, 23 μg at N l^{-1}, occurs on day 13 (not shown), two days after the wind stress falls to zero. As upwelling decays further (Fig. 15a), primary productivity declines (Fig. 15b) and the phytoplankton maximum recedes toward the coast, deepens, and diminishes (Fig. 15c).

After 20 days the plant maximum has decreased to 15.4 μg at N l^{-1} and occurs contiguous with the coast at a depth of 15 m (Fig. 16c). With no wind forcing, upwelling has all but ceased (Fig. 16a) and primary productivity approaches nutrient-limited values (Fig. 16b). Surface waters move shoreward (Fig. 15a and 16a) carrying the zooplankton standing stock closer to shore (not shown). The detritus maximum decays (not shown) as fecal pellet production lessens. The ammonia maximum wanes (also not shown) as more NH_4 is oxidized to NO_3 than is added by decomposing fecal pellets.

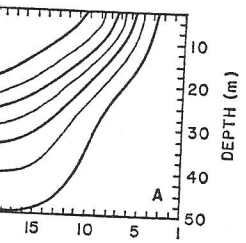

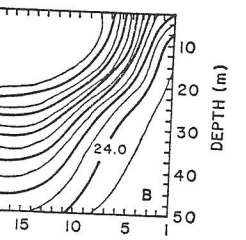

(a) The zooplankton field. Contour in-
ntour intervals are 2 μg at NO_3 l^{-1}.

an ammonia maximum exists at a
re (Fig. 14b). The ammonia input
slower oxidation of ammonia into
this region.

plankton plume. As the wind stress
coastal upwelling and the offshore
n the newly upwelled water remain
ncentration, 23 μg at N l^{-1}, occurs
stress falls to zero. As upwelling
leclines (Fig. 15b) and the phyto-
pens, and diminishes (Fig. 15c).
ed to 15.4 μg at N l^{-1} and occurs
. 16c). With no wind forcing, up-
productivity approaches nutrient-
shoreward (Fig. 15a and 16a)
shore (not shown). The detritus
roduction lessens. The ammonia
s oxidized to NO_3 than is added

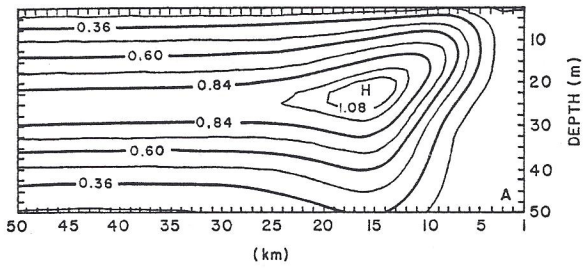

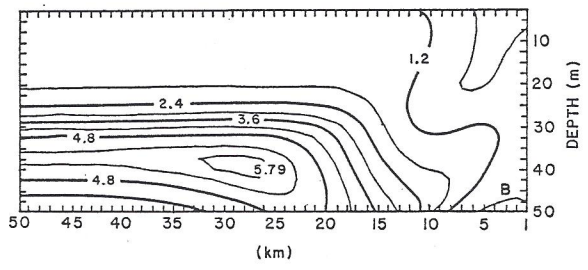

Figure 14. The strong upwelling case, after 10 days: (a) The distribution of detritus. Contour intervals are 0.12 μg at N l^{-1}. (b) The ammonia field. Contour intervals are 0.6 μg at NH_4 l^{-1}.

c. Daily primary production of the water column during the strong upwelling case. Figure 17 summarizes the relationship between the north-south component of the wind stress and daily primary production. The maximum production occurs on day 10 at 5 km from shore (Fig. 12b) where upwelling of nutrients is strong and plant standing crop is high. The increasing amplitude of the production curve in Figure 17 reflects both the growing concentration of phytoplankton and the increasing supply of nutrients. Production rapidly declines when the wind stress decays on day 11. With no further wind forcing of upwelling, phytoplankton growth becomes nutrient limited (Fig. 17).

d. Plume structure and daily primary production during intermittent upwelling. To simulate the response of primary production to intermittent upwelling, Thompson's (1974) numerical model was run with a time dependent wind stress calculated from the August, 1973, recordings of an anemometer located at Newport, Oregon. The circulation model was driven from rest on August 1 with initial conditions specified from observational hydrographic data. Initial conditions for the biological dependent variables were the same as for the strong upwelling case, namely the steady state solution of the (x,z,t) ecosystem model in the absence of advection.

The distributions of the dependent variables (P, Z, NO_3, NH_4 and D) all develop

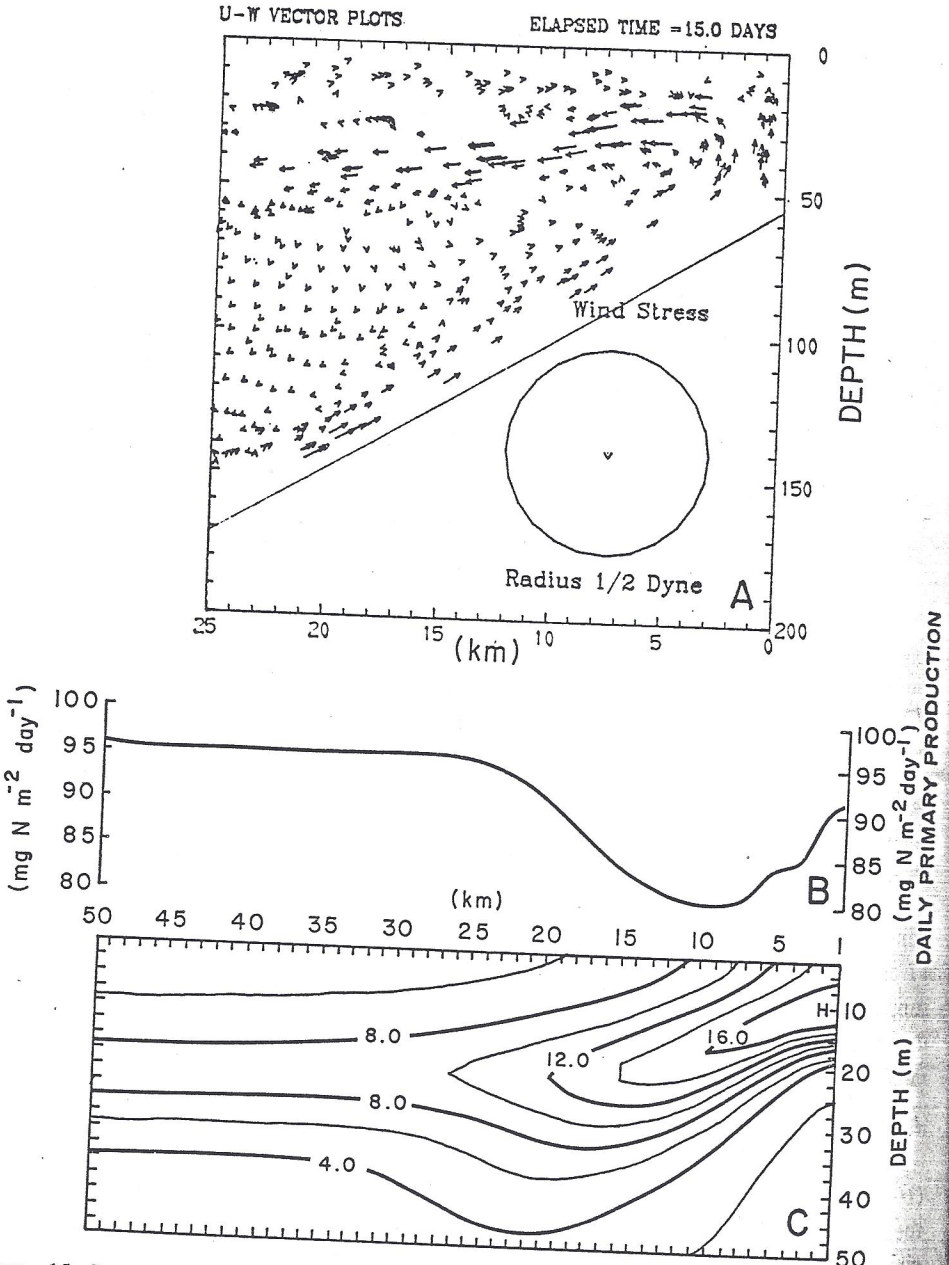

Figure 15. Same as Fig. 10 but after 15 days. The maximum u and w velocities in (a) are -3.6 cm sec^{-1} and 1.5×10^{-2} cm sec^{-1}, respectively. Contour intervals in (c) are 2.0 μg at N l^{-1}.

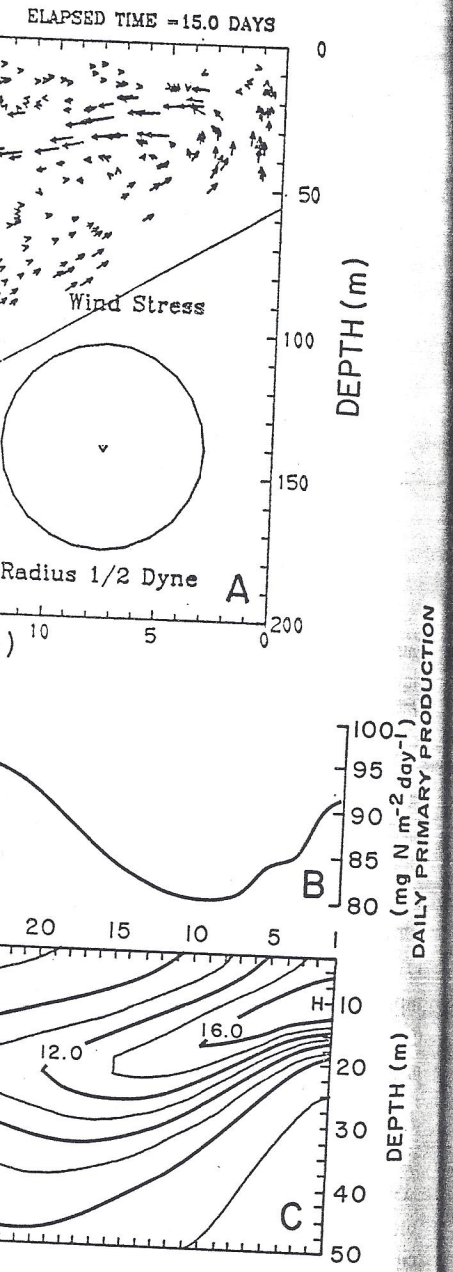

maximum u and w velocities in (a) are
ely. Contour intervals in (c) are 2.0 μg at

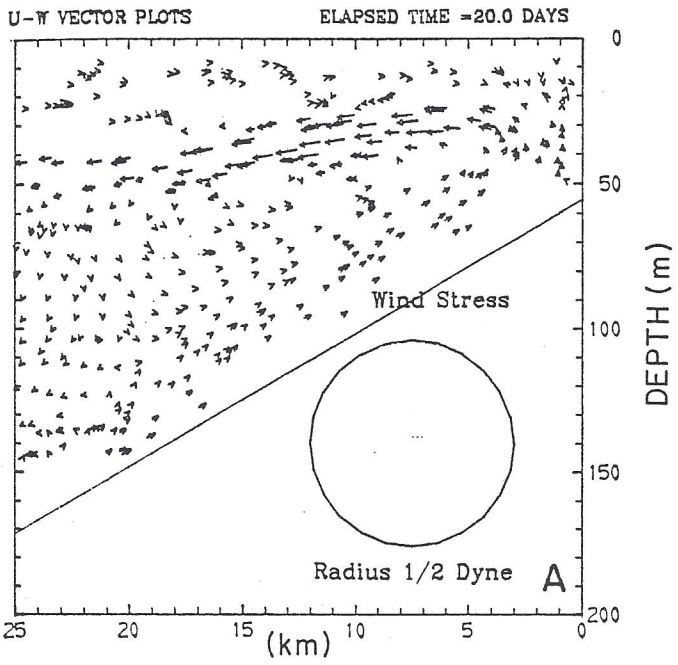

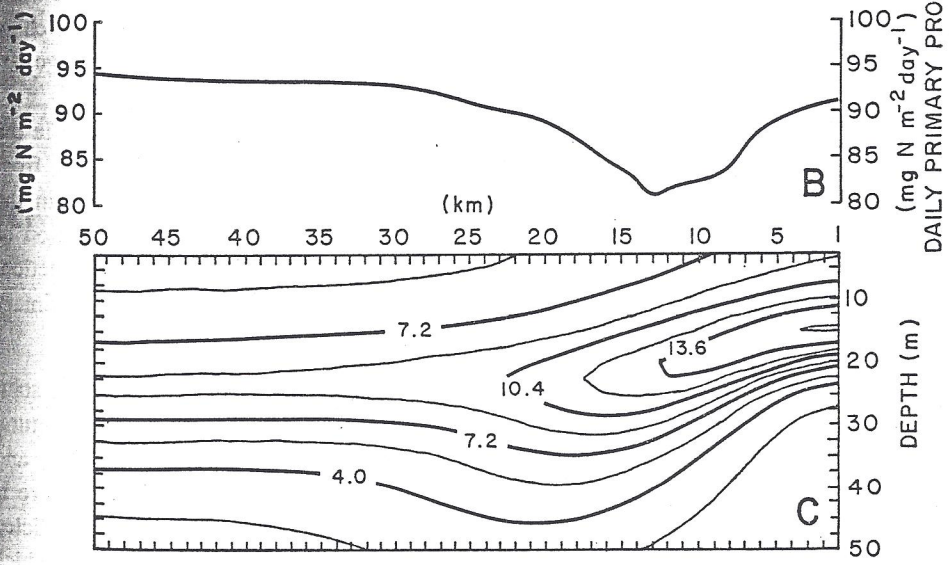

Figure 16. Same as Fig. 10 but after 20 days. The maximum u and w velocities in (a) are -2.8 cm sec^{-1} and 7.9×10^{-3} cm sec^{-1}, respectively. Contour intervals in (c) are 1.6 μg at N l^{-1}.

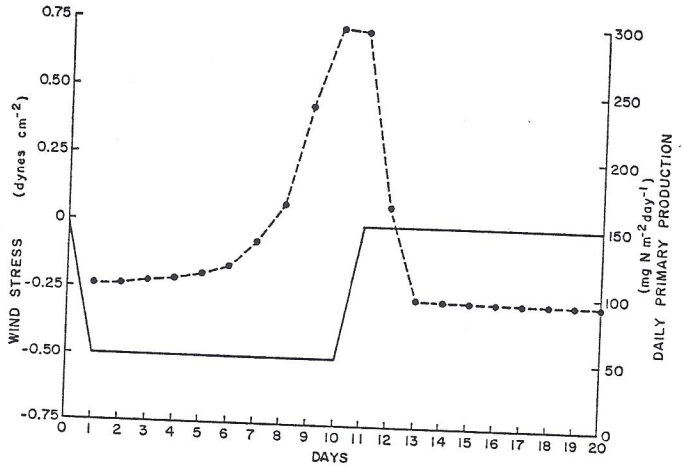

Figure 17. The north-south component of the wind stress (solid line) near the coast for the strong upwelling case. The data points (dashed line) represent the maximum daily gross primary production calculated for each model day.

features during intermittent upwelling similar to those found in the strong upwelling case. The phytoplankton plumes predicted for August 5 and August 15 are shown in Figure 18. A two-cell circulation (not shown) develops during early August when the wind stress (Fig. 19) is similar in magnitude to that of the strong upwelling case (Fig. 17). The circulation decays into a more confused flow after August 6 when periods of prolonged relaxation of the winds occur (Fig. 19).

While primary production steadily increased with continuous wind forcing in the strong upwelling case (Fig. 17), calculations of daily primary production from August 5 to August 20 show a variability which is related to fluctuations in the north-south component of the wind stress (Fig. 19). Each major intensification of the northerly wind component is followed by an increase in primary production. Upon relaxation of the wind stress, the rate of upwelling slows and the primary production decreases.

e. Comparison with observations. Many of the features in the (x,z,t) model solutions have been observed during CUE or have been described in the literature. Comparison of nitrate distributions measured by Ball (1970), Atlas (1973), and Myers (1975) with model simulations show good qualitative agreement. There is insufficient data, however, to validate the offshore ammonia maximum predicted by the model (Fig. 14b). The NH_4 maximum is a local, temporary feature which may be easily missed in field sampling.

Figure 20 shows the development of a phytoplankton plume off Newport, Oregon in August, 1972. The similarity in orientation, position and length scale between the simulated (Figs. 12c and 18a and b) and observed plume structure

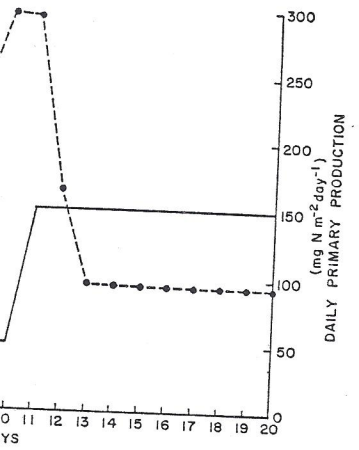

wind stress (solid line) near the coast for the
hed line) represent the maximum daily gross
day.

lar to those found in the strong upwelling
for August 5 and August 15 are shown
own) develops during early August when
gnitude to that of the strong upwelling
o a more confused flow after August 6
winds occur (Fig. 19).
ised with continuous wind forcing in the
ons of daily primary production from
which is related to fluctuations in the
(Fig. 19). Each major intensification of
by an increase in primary production.
te of upwelling slows and the primary

the features in the (x,z,t) model solu-
have been described in the literature.
ed by Ball (1970), Atlas (1973), and
good qualitative agreement. There is
offshore ammonia maximum predicted
m is a local, temporary feature which

phytoplankton plume off Newport,
orientation, position and length scale
and b) and observed plume structure

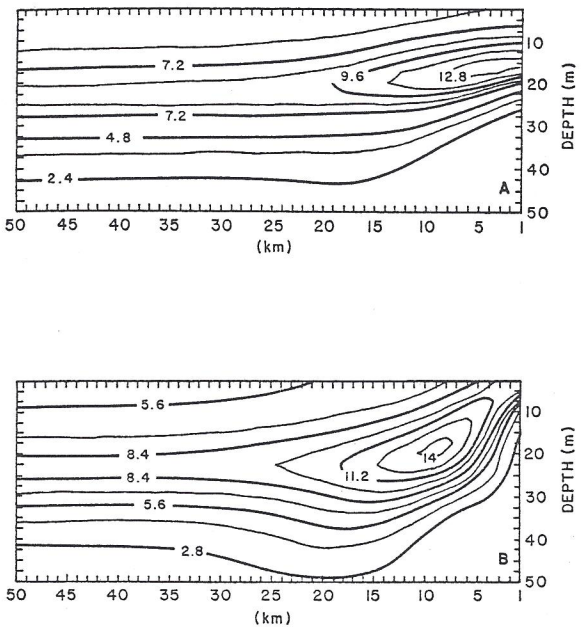

Figure 18. The intermittent upwelling case. (a) The distribution of phytoplankton on August 5. Contour intervals are 1.2 μg at N l^{-1}. (b) Same as (a) but on August 15. Contour intervals are 1.4 μg at N l^{-1}.

(Fig. 20) is striking. Turbidity measurements made by Pak *et al.* (1970) in June, 1967, indicate a suspended particle maximum existed within the same depth range and offshore location as the phytoplankton and detritus maxima shown in Figures 12c and 14a. To explain this particle distribution, they proposed a sequence of events in which nutrient rich water upwells close to shore, becomes increasingly

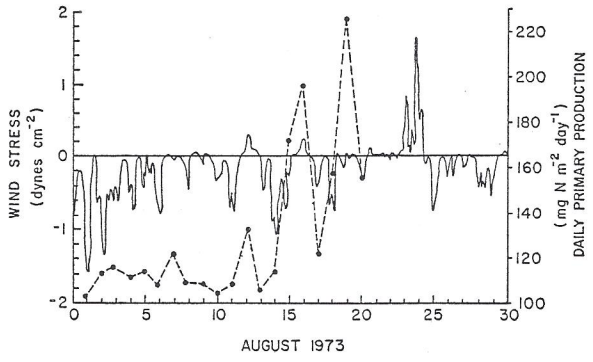

Figure 19. The north-south component of the wind stress (solid line) calculated from Newport, Oregon anemometer data recorded during August, 1973. The data points (dashed line) represent the maximum daily gross primary production predicted for the first 20 days.

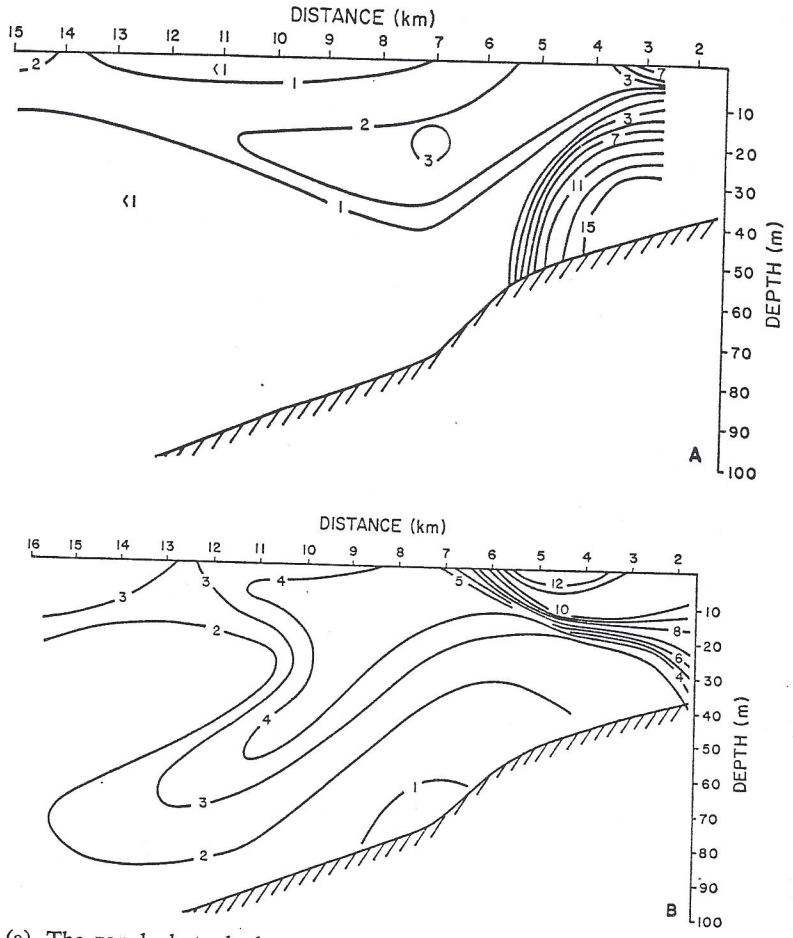

Figure 20 (a). The zonal phytoplankton distribution observed off Newport, Oregon on August 7, 1972. Plant biomass is expressed as mg chlorophyll *a* m^{-3}. (b) Same as (a) except observed on August 9, 1972 (data of L. F. Small).

concentrated with particles of biological origin as it moves offshore, and gradually sinks below the permanent pycnocline which slopes up to near the surface. This mechanism was adopted by Small and Ramberg (1971) and by Anderson (1972) to explain the plume feature often observed in the phytoplankton distribution during upwelling. Kitchen *et al.* (1975) suggest the particle maximum in July, 1973, was composed mostly of diatoms nearshore, which were progressively replaced by dinoflagellates in the offshore nutrient-limited waters.

Field measurements of ^{14}C primary productivity performed by Anderson (1964) and Small *et al.* (1972) during upwelling off Oregon ranged from 0.5 to 1.5 g *C* m^{-2} day^{-1}. If a C/N ratio of 7 is assumed (Small and Ramberg, 1971) the observed range in terms of nitrogen is 71 to 214 mg N m^{-2} day^{-1}. Gross primary

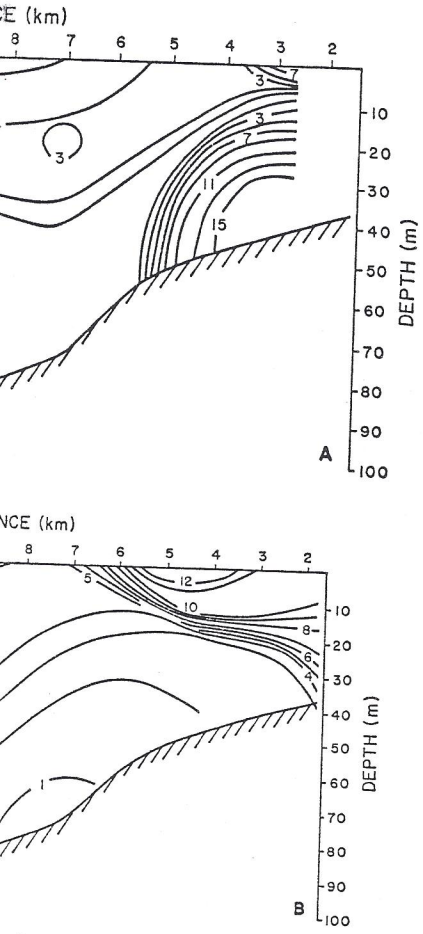

ution observed off Newport, Oregon on August chlorophyll *a* m^{-3}. (b) Same as (a) except ob-).

origin as it moves offshore, and gradually hich slopes up to near the surface. This amberg (1971) and by Anderson (1972) ed in the phytoplankton distribution dur- t the particle maximum in July, 1973, was which were progressively replaced by ed waters.

ductivity performed by Anderson (1964) off Oregon ranged from 0.5 to 1.5 g *C* ed (Small and Ramberg, 1971) the ob- 214 mg N m^{-2} day^{-1}. Gross primary

Table 1. Parameter values of the (x,z,t) ecosystem model.

Parameter	Value	Parameter	Value
a	4.09×10^{-1}	V_m	2.4×10^{-5} sec^{-1}
b	1.07	w_s	1.0×10^{-2} cm sec^{-1}
c	$1.0°C^{-1}$	W	2.0×10^{-2} cm sec^{-1}
d	4.32×10^{4} sec	Δx	1.0×10^{5} cm
E_m	1×10^{-6} sec^{-1}	Δz	2.5×10^{2} cm
H	5.0×10^{3} cm	Γ	2.4×10^{-6} sec^{-1}
I_s	1.2×10^{-3} cal cm^{-2} sec^{-1}	Δ	2.1×10^{-7} sec^{-1}
I_m	2.1×10^{-2} cal cm^{-2} sec^{-1}	η	4.30
K_h	5.0×10^{5} cm^2 sec^{-1}	θ	0.175
K_v	1.0 cm^2 sec^{-1}	κ_p	9.5×10^{-2} cm^2 (μg at N)$^{-1}$
k_u	1.0 μg at N l^{-1}	κ_w	6.7×10^{-4} cm^{-1}
L	5.0×10^{6} cm	Λ	0.06 (μg at N/l)$^{-1}$
N_t	30.0 μg at N l^{-1}	Ξ	1.2×10^{-6} sec^{-1}
P_t	0.0 μg at N l^{-1}	Υ	0.15 (μg at N/l)$^{-1}$
R_m	5.6×10^{-6} sec^{-1}	Φ	1.2×10^{-5} sec^{-1}
Δt	8.6×10^{2} sec	Ψ	1.46 (μg at N/l)$^{-1}$
U	10.0 cm sec^{-1}	Ω	4.7×10^{-7} sec^{-1}

productivities calculated by the model range between 78 and 296 mg N m^{-2} day^{-1} during the strong upwelling case, and from 78 to 226 mg N m^{-2} day^{-1} during the intermittent upwelling case. While the ^{14}C technique yields estimates closer to net production (Eppley and Sloan, 1965), the numbers are still comparable.

Model predictions of increased daily gross primary production of the water column after intensification of northerly winds (Figs. 17 and 19) are supported by CUE productivity data (Small, in preparation). The bloom of phytoplankton upon relaxation of strong winds (Section 4b) is a model feature clearly observed during the CUE field study.

Peterson (1972) observed that zooplankton standing stock was greater in the oceanic region than on the continental shelf off Oregon in summer. The model solutions (Fig. 13a) also show this distribution and indicate offshore water transport may lead to a low coastal herbivore biomass. Peterson and Miller (1975) found high zooplankton standing stocks near the coast during the 1969-71 upwelling seasons, as did Myers (1975) in August, 1973. Biomass was highest within 2 km of the beach, suggesting the source of these animals was the coastal populations. If the (x,z,t) model had included in its coastal boundary conditions an inshore source of zooplankton, or if zooplankton were allowed to migrate vertically to depths where onshore flow occurs, the observations of Peterson and Miller (1975) and Myers (1975) would have been more closely reproduced.

f. Model sensitivity analysis. The (x,z,t) model contains 34 independent or specified parameters (Table 1). The ideal method of parameter value investigation is an analytical sensitivity analysis. However, the theory of sensitivity analysis is well

developed only for steady state, one-box models (Tomovic, 1963). For the present, one must resort to an empirical sensitivity analysis for complex spatial models, such as the one described here. An empirical analysis begins with the best estimate for all parameter values; the model's response to variation of an individual parameter is then investigated. The following summarizes such an analysis of the (x,z,t) model.

The distributions of the dependent variables (P, Z, NO_3, NH_4 and D) are quite sensitive to the value of the vertical diffusion coefficient, K_v. With an increased value of K_v, the phytoplankton plume deepens as its vertical gradient is smoothed. Nutrients are supplied to the euphotic zone by vertical diffusion at a faster rate and daily gross primary production of the water column increases. The model is less responsive to an increase in the horizontal diffusion coefficient, K_h.

The response of primary production to variation in the temperature field was explored by assuming no offshore gradient in temperature. With 14°C surface temperatures at the coast, daily gross primary production on day 10 in the strong upwelling case increased by 65%. The phytoplankton plume occurred closer to the coast and to the surface, and the plant biomass increased by 2 μg at N l^{-1} over the maximum concentration shown in Figure 12c. Thus a proper specification of the temperature field is necessary to prevent overestimation of primary production.

Phytoplankton production is also quite sensitive to the availability of light. Greater incident radiation at the surface results in both an enhancement of the light inhibition effect and an increase in daily primary production. The depth of the euphotic zone does not increase as the dense phytoplankton bloom becomes self-shading. Only a reduction in the self-shading coefficient, κ_p, or the light extinction coefficient, κ_w, would allow an increased euphotic zone depth. An increase in the senescent cell lysis coefficient, Ξ, would lower the concentration of plants in the aphotic zone.

An increase in the detritus sinking velocity, w_s, causes a deepening of the maximum in both the detritus and ammonia distributions, and a more rapid loss of limiting nutrient from the euphotic zone in the form of decomposing fecal pellets. The detritus regeneration rate parameter, Φ, and the ammonia oxidation rate parameter, Ω, have long e-folding rates, yet their values are important. Increasing Φ liberates more ammonia for plant growth in the euphotic zone. Increasing Ω can prevent the development of a NH_4 maximum in the spatial solutions.

Empirical analysis of (9)-(13) shows the parameters describing zooplankton grazing, egestion and excretion are the most important relative to the phytoplankton growth rate, V_m, in determining the steady state concentrations of P, Z, NO_3, NH_4 and D. These nonspatial equations have a stable solution with P^* set to zero. Likewise, a positive grazing threshold is unnecessary to prevent phytoplankton extinction in the spatial model. Diffusion of plants from areas of high concentration to low concentration keeps a finite amount of plant standing crop present at each grid

point. Yet P_t can act as a parameterization of turbulent diffusion in nonspatial models (Wroblewski and O'Brien, 1976).

5. Summary, conclusions and critique

The goal of this research has been to provide a dynamical explanation for the spatial features which are consistently observed in the particulate nitrogen distribution during upwelling conditions off Oregon. The similarity between simulations and field data, while not a conclusive verification of the model, suggests the model may include the basic biological and physical dynamics governing primary production during a strong upwelling event.

The dominant role of advection in determining the spatial configuration of plankton and nutrient fields in upwelling regions is obvious from the model solutions. The physical mechanism which leads to the phytoplankton plume observed over the continental shelf off Oregon appears to be that suggested by Pak *et al.* (1970), and described dynamically by Mooers *et al.* (1976). The numerical upwelling model of Thompson (1974) simulates this circulation (i.e. upwelling at the coast, offshore transport and downwelling in the region 6 to 20 km offshore). This physical process, when coupled to the biological dynamics formulated in Section 2, produces the phytoplankton plume. However, the distribution of the phytoplankton may differ appreciably from the plume structure under a different wind regime and upwelling circulation pattern.

In spite of the successful reproduction of several observed biological and chemical features, this model is fundamentally limited in its ability to predict the distribution of nitrogen in time and space. Numerical solutions of a nonlinear, dissipative, open thermodynamic system (such as the Oregon upwelling system) will diverge from the "real" solution if the initial state of the system is not known exactly (Lorenz, 1969). The inevitable discrepancy between model prediction and observation stems from the fact that continuous oceanic processes are represented by finite approximations. Platt *et al.* (1977) estimate the limit to predictability of planktonic features with a 10 km length scale is at best several days. After this period, the numerical solution and the observed field may differ appreciably.

An important criticism of this model is the assumption that all parameter values have no spatial or temporal dependence. The carnivore trophic level is ignored in the biological dynamics. Zooplankton are advected and diffused as passive drifters, disregarding the swimming ability of these animals. Longshore variation in all model variables has been neglected, even though conservation of mass in the zonal plane is not achieved during Oregon upwelling (Peffley and O'Brien, 1976). The model also ignores the possible influence of the Columbia River effluent tongue upon the physical and chemical environment off Oregon.

Still, this model represents the most complex formulation of an upwelling ecosystem. Its major strength is the integration of numerous physical and biological

processes. A major weakness is the treatment of individual phytoplankton and zooplankton species as members of a food chain with invariable tropho-dynamic relationships. Few organisms play such a simple structured role in nature.

Acknowledgments. This work was supported by the Office of Naval Research under Contract N00014-67-A-0235 while the author was a doctoral student at Florida State University. The NSF-International Decade of Ocean Exploration provided partial support through the Coastal Upwelling Ecosystems Analysis program under National Science Foundation Grant No. GX-33502. The author was awarded a NSF Grant for Improving Doctoral Dissertation Research, Grant No. GA-43265. The National Center for Atmospheric Research, Boulder, Colorado awarded the author a Computing Facilities Grant in support of this research. NCAR is sponsored by NSF. Computations were also performed on the CDC 6400 at FSU.

The accomplishment of this work would not have been possible without the cooperation and encouragement of Dr. J. D. Thompson, who provided the physical component of this investigation in a serious effort at interdisciplinary research. I thank Drs. J. J. O'Brien, R. L. Iverson, L. F. Small, G. A. Knauer and T. G. Hallam for many suggestions and stimulating dialogues. Drs. L. F. Small and C. B. Miller of Oregon State University provided observational data collected during the Coastal Upwelling Experiment.

This is a contribution to the CUEA program of NSF.

APPENDIX. Definition of symbols and scaling relationships

Dimensional Quantity	Definition	Scaling Factor	Nondimensional Quantity
—	Temperature function parameters	—	a,b
c	Temperature function parameter	—	—
D	Detrital nitrogen	D/N_t	D'
d	Daylength fraction of a day	—	—
E_m	Maximum herbivore egestion coefficient	E_m/V_m	ρ
H	Characteristic vertical length scale	—	—
I_s	Light saturation parameter when $\theta = 0$ or $\eta = 0$	—	—
I_m	Light intensity at local apparent noon	—	—
K_h	Horizontal eddy diffusivity	—	—
K_v	Vertical eddy diffusivity	—	—
k_u	Half-saturation constant for nutrient uptake	k_u/N_t	α
L	Characteristic horizontal length scale	—	—
NH_4	Ammonia	NH_4/N_t	NH_4'
NO_3	Nitrate plus nitrite	NO_3/N_t	NO_3'
N_t	Total concentration of biologically limiting nutrient	—	—
P	Phytoplankton nitrogen	P/N_t	P'
P_t	Herbivore grazing threshold	P_t/N_t	P^*
R_m	Herbivore maximum grazing rate	R_m/V_m	β
T	Temperature	—	—
t	Time	tV_m	τ
u	x-directed velocity component	u/U	u'

Dimensional Quantity	Definition	Scaling Factor	Nondimensional Quantity
U	Typical value of the horizontal velocity	—	—
V_m	Phytoplankton maximum nutrient uptake rate	—	—
W	Typical value of the vertical velocity	—	—
w	z-directed velocity component	w/W	w'
w_s	Sinking velocity of detritus	w_s/W	w_s'
x	Tangent-plane Cartesian coordinate: x positive toward the coast	x/L	x'
Z	Zooplankton nitrogen	Z/N_t	Z'
z	Tangent-plane Cartesian coordinate: z positive upward	z/H	z'
Γ	Herbivore excretion coefficient	Γ/V_m	γ
Δ	Herbivore egestion rate at phytoplankton concentration P_t	Δ/V_m	δ
—	Light function parameters	—	η,θ
κ_p	Light extinction per unit phytoplankton nitrogen	—	—
κ_w	Light extinction coefficient of pure seawater and any nonphytoplanktonic material	—	—
Λ	Ivlev constant	ΛN_t	λ
μ_m	Phytoplankton maximum growth rate	—	—
Ξ	Phytoplankton nutrient loss coefficient	Ξ/V_m	ξ
—	Pi	—	Π
Υ	Herbivore egestion coefficient	ΥN_t	ν
Φ	Detritus decomposition parameter	Φ/V_m	ϕ
Ψ	Nitrate uptake inhibition parameter	ΨN_t	ψ
Ω	Ammonia oxidation coefficient	Ω/V_m	ω

REFERENCES

Anderson, G. C. 1964. The seasonal and geographic distribution of primary productivity off the Washington and Oregon coasts. Limnol. Oceanogr., *9*, 284–302.

—— 1972. Aspects of marine phytoplankton studies near the Columbia River, with special reference to a subsurface chlorophyll maximum, *in* The Columbia River Estuary and Adjacent Ocean Waters, A. T. Pruter and D. L. Alverson, eds., Seattle, Univ. of Washington Press, 219–240.

Anita, N. J., C. D. McAllister, T. R. Parsons, K. Stephens and D. H. Strickland. 1963. Further measurements of primary production using a large-volume plastic sphere. Limnol. Oceanogr., *8*, 166–183.

Atlas, E. L. 1973. Changes in chemical distributions and relationships during an upwelling event off the Oregon coast. M. S. thesis. Oregon State Univ., Corvallis, 100 pp.

Ball, D. S. 1970. Seasonal distribution of nutrients off the coast of Oregon, 1968. M. S. thesis. Oregon State Univ., Corvallis, 71 pp.

Barber, R. T. and J. H. Ryther. 1969. Organic chelators: factors affecting primary production in the Cromwell current upwelling. J. exp. mar. Ecol., *3*, 191–199.

Beers, J. R., W. R. Stevenson, R. W. Eppley and E. R. Brooks. 1971. Plankton populations and upwelling off the coast of Peru, June 1969. Fish. Bull., *69*, 859–876.

Caperon, J. and J. Meyer. 1972. Nitrogen-limited growth of marine phytoplankton—II. Uptake kinetics and their role in nutrient limited growth of phytoplankton. Deep-Sea Res., *19*, 619–632.

Conover, R. 1966. Factors affecting the assimilation of organic matter by zooplankton and the question of superfluous feeding. Limnol. Oceanogr., *11*, 346-354.

Corner, E. D. S. and A. G. Davies. 1971. Plankton as a factor in the nitrogen and phosphorus cycles in the sea. Adv. mar. Biol., *9*, 101–204.

Corner, E. D. S., C. B. Cowey and S. M. Marshall. 1965. On the nutrition and metabolism of zooplankton. III. Nitrogen excretion by *Calanus*. J. Mar. Biol. Ass. U. K., *45*, 429–442.

Cushing, D. H. 1971. Upwelling and the production of fish. Adv. mar. Biol., *9*, 255–334.

Dugdale, R. C. 1967. Nutrient limitations in the sea: dynamics, identification, and significance. Limnol. Oceanogr., *12*, 685–695.

Dugdale, R. C. and J. J. MacIsaac. 1971. A computation model for the uptake of nitrate in the Peru upwelling region. Inv. Pesq., *35*, 299–308.

Eppley, R. W. 1972. Temperature and phytoplankton growth in the sea. Fish. Bull., *70*, 1063–1085.

Eppley, R. W. and J. J. Coatsworth. 1968. Uptake of nitrate and nitrite by *Ditylum brightwelli*—kinetics and mechanisms. J. Phycol., *4*, 151–165.

Eppley, R. W. and P. R. Sloan. 1965. Carbon balance experiments with marine phytoplankton. J. Fish. Res. Bd. Canada, *22*, 1083–1097.

Eppley, R. W., J. N. Rogers and J. J. McCarthy. 1969. Half-saturation constants for uptake of nitrate and ammonia by marine phytoplankton. Limnol. Oceanogr., *14*, 912–920.

Fee, E. J. 1969. A numerical model for the estimation of photosynthetic production, integrated over time and depth, in natural waters. Limnol. Oceanogr., *14*, 906–911.

Frost, B. W. 1974. Feeding processes at lower trophic levels in pelagic communities, *in* The Biology of the Oceanic Pacific, C. B. Miller, ed., Corvallis, Oregon State Univ. Press, 59–77.

Halpern, D. 1974. Observations of the deepening of the wind-mixed layer in the northeast Pacific Ocean. J. Phys. Oceanogr., *4*, 454–466.

Hurlburt, H. E. 1974. The influence of coastline geometry and bottom topography on the Eastern Ocean circulation. Ph.D. thesis, Florida State Univ., Tallahassee, 103 pp.

Ivlev, V. S. 1945. The biological productivity of waters. Usp. soverm. Biol., *19*, 98–120.

Johnston, R. 1964. Sea water, the natural medium of phytoplankton—II. Trace metals and chelation, and general discussions. J. Mar. biol. Ass. U. K., *44*, 87–109.

Kelley, J. C., T. E. Whitledge and R. C. Dugdale. 1975. Results of sea surface mapping in the Peru upwelling system. Limnol. Oceanogr., *20*, 784–794.

Kitchen, J. C., D. Menzies, H. Pak and J. R. V. Zaneveld. 1975. Particle size distributions in a region of coastal upwelling analyzed by characteristic vectors. Limnol. Oceanogr., *20*, 775–783.

Kullenberg, G. E. B. 1976. On vertical mixing and the energy transfer from the wind to the water. Tellus, *28*, 159–165.

Lorenz, E. N. 1969. The predictability of a flow which possesses many scales of motion. Tellus, *21*, 289–307.

MacIsaac, J. J. and R. C. Dugdale. 1969. The kinetics of nitrate and ammonia uptake by natural populations of marine phytoplankton. Deep-Sea Res., *16*, 45–57.

Mooers, C. N. K., C. A. Collins and R. L. Smith. 1976. The dynamic structure of the frontal zone in the coastal upwelling region off Oregon. J. Phys. Oceanogr., *6*, 3–21.

Mullin, M. M., E. F. Stewart, and F. J. Fuglister. 1975. Ingestion by planktonic grazers as a function of concentration of food. Limnol. Oceanogr., *20*, 259–262.

Myers, A. H. 1975. Vertical distribution of zooplankton in the Oregon coastal zone during an upwelling event. M. S. thesis. Oregon State Univ., Corvallis, 62 pp.

O'Brien, J. J. and J. S. Wroblewski. 1973. On advection in phytoplankton models. J. theor. Biol., *38*, 197–202.

—— 1976. A simulation of the mesoscale distribution of the lower marine trophic levels off West Florida, *in* Systems Analysis and Simulation in Ecology, Vol. 4, B. C. Patten, ed., New York, Academic Press, 63–110.

Okubo, A. 1971. Oceanic diffusion diagrams. Deep-Sea Res., *18*, 789–802.

Packard, T. T. and D. Blasco. 1974. Nitrate reductase activity in upwelling regions. II. Ammonia and light dependence. Tethys, *6*, 269–280.

Pak, H., G. F. Beardsley, Jr. and R. L. Smith. 1970. An optical and hydrographic study of a temperature inversion off Oregon during upwelling. J. Geophys. Res., *75*, 629–636.

Park, K. 1967. Nutrient regeneration and preformed nutrients off Oregon. Limnol. Oceanogr., *12*, 353–357.

Parsons, T. and M. Takahashi. 1973. Biological Oceanographic Processes. New York, Pergamon Press, 186 pp.

Parsons, T. R., R. J. LeBrasseur and J. D. Fulton. 1967. Some observations on the dependence of zooplankton grazing on cell size and concentration of phytoplankton blooms. J. Oceanogr. Soc. Japan, *23*, 10–17.

Peffley, M. B. and J. J. O'Brien. 1976. A three-dimensional simulation of coastal upwelling off Oregon. J. Phys. Oceanogr., *6*, 164–180.

Peterson, W. K. 1972. Distribution of pelagic copepods off the coast of Washington and Oregon during 1961 and 1962, *in* The Columbia River Estuary and Adjacent Waters, A. T. Pruter and D. L. Alverson, eds., Seattle, Univ. of Washington Press, 313–343.

Peterson, W. T. and C. B. Miller. 1975. Year-to-year variations in the planktology of the Oregon upwelling zone. Fish. Bull., *73*, 642–653.

Piacsek, S. A. and G. P. Williams. 1970. Conservation properties of convection difference schemes. J. Comp. Phys., *6*, 392–405.

Platt, T., K. L. Denman and A. D. Jassby. 1977. Modeling the productivity of phytoplankton, *in* The Sea, Vol. 6, E. D. Goldberg, ed., New York, John Wiley, 807–856.

Redfield, A. C., B. H. Ketchum and F. A. Richards. 1963. The influence of organisms on the composition of sea-water, *in* The Sea, Vol. 2, M. N. Hill, ed., New York, Wiley Interscience, 26–77.

Reed, R. K. and D. Halpern. 1974. Radiation measurements off the Oregon coast July/August 1973. Coastal Upwelling Ecosystems Analysis Data Report 13. Univ. of Washington, Seattle. 51 pp.

Ryther, J. H. 1956. Photosynthesis in the ocean as a function of light intensity. Limnol. Oceanogr., *1*, 61–70.

Shaffer, G. 1974. On the North West African coastal upwelling system. Ph.D. thesis. Institut für Meereskunde, Universitat Kiel, Federal Republic of Germany. 177 pp.

Small, L. F. and H. C. Curl, Jr. 1968. The relative contribution of particulate chlorophyll and river tripton to the extinction of light off the coast of Oregon. Limnol. Oceanogr., *13*, 84–91.

Small, L. F. and D. A. Ramberg. 1971. Chlorophyll *a*, carbon, and nitrogen in particles from a unique coastal environment, *in* Fertility of the Sea, Vol. 2, J. D. Costlow, Jr., ed., New York, Gordon and Breach, 475–492.

Small, L. F., H. Curl, Jr. and W. A. Glooschenko. 1972. Effects of solar radiation and upwelling on daily primary production off Oregon. J. Fish. Res. Bd. Canada, *29*, 1269–1275.

Smayda, T. J. 1966. A quantitative analysis of the phytoplankton of the Gulf of Panama. III.

General ecological conditions and the plankton dynamics at 8°45'N, 79°23'W from November 1954 to May 1957. Inter-Amer. Trop. Tuna Comm. Bull., *11*, 355–612.

—— 1969. Some measurements of the sinking rate of fecal pellets. Limnol. Oceanogr., *14*, 621–625.

Steele, J. H. 1974. The Structure of Marine Ecosystems. Cambridge, Mass., Harvard Univ. Press, 128 pp.

Thompson, J. D. 1974. The coastal upwelling cycle on a beta-plane: hydrodynamics and thermodynamics. Ph.D. thesis, Florida State Univ., Tallahassee, 141 pp.

Tomovic, R. 1963. Sensitivity Analysis of Dynamic Systems, New York, McGraw-Hill, 142 pp.

Vollenweider, R. A. 1965. Calculation models of photosynthesis-depth curves and some implications regarding day rate estimates in primary production measurements, *in* Primary Productivity in Aquatic Environments. Mem. Ist. Ital. Idrobiol., *18*, Suppl., C. R. Goldman, ed., Berkeley, Univ. of Calif. Press, 425–457.

Von Brand, T., N. W. Rakestraw and C. E. Renn. 1937. The experimental decomposition and regeneration of nitrogenous organic matter in seawater. Biol. Bull., *72*, 165–175.

Von Brand, T. and N. W. Rakestraw. 1940. Decomposition and regeneration of nitrogenous organic matter in sea water. III. Influence of temperature and source and condition of water. Biol. Bull., *79*, 231–236.

Walsh, J. J. 1975. A spatial simulation model of the Peru upwelling ecosystem. Deep-Sea Res., *22*, 201–236.

Walsh, J. J. and R. C. Dugdale. 1971. A simulation model of the nitrogen flow in the Peruvian upwelling system. Inv. Pesq., *35*, 309–330.

—— 1972. Nutrient submodels and simulation models of phytoplankton production in the sea, *in* Nutrients in Natural Waters, J. Kramer and H. Allen, eds., New York, J. Wiley and Sons, 171–191.

Walsh, J. J., J. C. Kelley, T. E. Whitledge and J. J. MacIsaac. 1974. Spin up of the Baja California upwelling ecosystems. Limnol. Oceanogr., *19*, 553–572.

Winter, D. F., K. Banse and G. C. Anderson. 1975. The dynamics of phytoplankton blooms in Puget Sound, a fjord in the Northwestern United States. Mar. Biol., *29*, 139–176.

Wroblewski, J. S. 1976. A model of the spatial structure and productivity of phytoplankton populations during variable upwelling off the coast of Oregon. Ph.D. thesis, Florida State Univ., Tallahassee, 116 pp.

Wroblewski, J. S. and J. J. O'Brien. 1976. A spatial model of phytoplankton patchiness. Mar. Biol., *35*, 161–175.

Yentsch, C. S. and R. W. Lee. 1966. A study of photosynthetic light reactions, and a new interpretation of sun and shade phytoplankton. J. Mar. Res., *24*, 319–337.

Received: *31 August, 1976;* revised: *27 February, 1977.*